Yao, H., Ibayashi, S., Sugimori, H., Fujii, K., Fujishima, M., 1996. Simplified model of krypton laser-induced thrombotic distal middle cerebral artery occlusion in spontaneously hypertensive rats. Stroke 27, 333–336.

Yenari, M.A., Fink, S.L., Sun, G.H., Chang, L.K., Patel, M.K., Kunis, D.M., Onley, D., Ho, D.Y., Sapolsky, R.M., Steinberg, G.K., 1998. Gene therapy with HSP72 is neuroprotective in rat models of stroke and epilepsy. Ann. Neurol. 44, 584–591.

Yenari, M.A., Minami, M., Sun, G.H., Meier, T.J., Kunis, D.M., McLaughlin, J.R., Ho, D.Y., Sapolsky, R.M., Steinberg, G.K., 2001. Calbindin d28k overexpression protects striatal neurons from transient focal cerebral ischemia. Stroke 32, 1028–1035.

Zabner, J., Couture, L.A., Gregory, R.J., Graham, S.M., Smith, A.E., Welsh, M.J., 1993. Adenovirus-mediated gene transfer transiently corrects the chloride transport defect in nasal epithelia of patients with cystic fibrosis. Cell 75, 207–216.

ELSEVIER

Experimental Gerontology 38 (2003) 423–429

Experimental Gerontology

www.elsevier.com/locate/expgero

Adenovirus-mediated gene transfer to ischemic brain is augmented in aged rats

Junichi Takada*, Hiroaki Ooboshi, Hiroshi Yao, Takanari Kitazono, Setsuro Ibayashi, Mitsuo Iida

Department of Medicine and Clinical Science, Graduate School of Medical Sciences, Kyushu University, Maidashi 3-1-1, Higashi-ku, Fukuoka 812-8582, Japan

Received 9 August 2002; received in revised form 10 October 2002; accepted 22 October 2002

Abstract

Gene therapy may be a promising approach for the treatment of brain ischemia. Because older populations are susceptible to ischemic stroke, we examined the effects of aging on adenovirus-mediated gene transfer to the ischemic brain of rats. Brain ischemia was produced by photochemical occlusion of the distal middle cerebral artery of aged and adult spontaneously hypertensive rats. Ninety minutes after ischemia, an adenoviral vector encoding β-galactosidase was injected into the contralateral (C) and ipsilateral [peri-ischemic (I-p) and ischemic core (I-c)] parietal cortices. Cerebral blood flow (CBF) was measured by laser Doppler flowmetry. Transgene expression was scored semiquantitatively as an expression score by histochemistry and also quantitatively analyzed by chemiluminescence assay. Changes in CBF after ischemia in aged rats were not significantly different from those in adult rats, although the infarct rim in the older rats tended to be closer to the midline than in the younger rats. β-galactosidase was detected in both neurons and non-neuronal cells at C and I-p, and was primarily present in non-neuronal cells at I-c. The expression scores 1 and 4 days after ischemia in the aged rats were similar to those in the adult rats. However, the score for the I-c at 7 days after injection was significantly greater in the older rats than in the younger adult rats. β-galactosidase activity at I-c 7 days after ischemia in the aged rats (8.0 ± 1.7 mU/mg protein) was significantly greater than that in the adult rats (1.3 ± 0.4, $p < 0.01$). Adenovirus-mediated gene transfer to the ischemic brain may thus be more effective in aged rats than in adult rats.

Keywords: Gene transfer; Aging; Adenoviral vector; Brain ischemia

1. Introduction

Gene transfer is a promising method for the treatment of cardiovascular disease. Several clinical gene therapy trials for cardiovascular disease have been undertaken, some of which have shown good outcomes (Abbott, 2001). Gene therapy as a treatment of cerebrovascular disease may also prove to be an attractive application (Heistad and Faraci, 1996; Ooboshi et al., 1995a). Some experimental studies have demonstrated the efficacy of gene therapy for brain ischemia in which non-viral and viral vectors, including adenovirus (Betz et al., 1995; Xu et al., 1997; Yang et al., 2001), were used for gene delivery. We have recently shown that adenovirus-mediated gene transfer to the ischemic brain provides an effective level of transgene expression in non-ischemic and even in peri-ischemic or penumbra areas (Ooboshi et al., 2001).

Stroke is the leading cause of death in the elderly population (Ueda et al., 1990), and brain infarction is the most common type of stroke in Japan. In addition, aging is one of the major risk factors for cerebrovascular diseases. It is therefore important to study ischemic stroke using aged animals (Millikan, 1992; Futrell et al., 1991; Yao et al., 1991; Ooboshi et al., 1995b; Davis et al., 1995). However, such studies of gene therapy are few. Therefore, in the present study, we examined whether aging would affect the transgene expression in the context of adenoviral vector-mediated gene transfer to the ischemic brain.

2. Material and methods

2.1. Adenovirus preparation

We used a replication-deficient recombinant adenovirus carrying bacterial β-galactosidase (AdCMVβGal) as

* Corresponding author. Fax: +81-92-642-5271.
E-mail address: takada@intmed2.med.kyushu-u.ac.jp (J. Takada).

0531-5565/03/$ - see front matter © 2002 Elsevier Science Inc. All rights reserved.
PII: S0531-5565(02)00241-3

the reporter gene. Generation of AdCMVβGal has previously been described (Davidson et al., 1993; Davidson et al., 1994). Viral titers were determined by plaque assay using HEK 293 cells. After purification, the virus was suspended in phosphate-buffered saline (PBS) with 3% sucrose, and was kept at −80 °C until used for the experiment.

2.2. Animals and surgical procedure

All animal procedures were approved by the Animal Care and Use Review Committee at Kyushu University. Seventeen female spontaneously hypertensive adult rats (SHR; age: 5–7 months; weight: 204–244 g) and 17 female aged SHR (age: 19–21 months; weight: 208–254 g) were used for the present study. Surgical procedures used in this study were performed as previously described (Ooboshi et al., 2001). Rats were anesthetized with halothane (3% for induction, and 1.5% during the surgical preparation with a face mask, 0.75% after intubation, and 0.5% for maintenance). The right femoral artery and vein were cannulated for monitoring mean arterial pressure (MAP) or sampling blood, and for the injection of agents, respectively. The rats were endotracheally intubated, and mechanically ventilated after intravenous injection of pancuronium bromide (an initial dose of 0.3 mg followed by 0.1 mg every 60 min). Rectal and head temperature was maintained at 37 and 36 °C, respectively, by means of a heating pad and a warming lamp. Rats were mounted on a stereotaxic head holder, and burr holes were drilled in the bilateral parietal cortices and the right temporal cortex. Cerebral blood flow (CBF) was measured by laser Doppler flowmetry (ALF21, ADVANCE Co. Ltd, Japan) at 2.7 mm lateral and 1.5 mm posterior to the bregma contralateral to the ischemic side (C: contralateral control area), and at 2.7 mm (I-p: peri-ischemic area) and 4 mm lateral (I-c: ischemic core area) in the ipsilateral side.

2.3. Brain ischemia and injection of adenoviral vector

Brain ischemia was produced by photochemical occlusion of the distal middle cerebral artery (MCA), as described previously (Yao et al., 1996). A krypton laser (Innova 301, Coherent Inc., Palo Alto, CA) was used to irradiate the distal MCA at a power of 20 mW. The photosensitizing dye rose bengal (15 mg/ml in 0.9% saline; Wako Pure Chemical, Japan) was administered intravenously to a body dose of 20 mg/kg over 90 s simultaneously with 4 min of laser irradiation. Ninety minutes after the distal MCA occlusion, 5 μl of viral suspension (3×10^{10} plaque forming units/ml) was injected into the parietal regions, where blood flow was measured (C, I-p, and I-c regions) over 10 min (Ooboshi et al., 2001). The burr holes were then covered with bone wax, and the scalp was sutured. The rats were carefully weaned from the respirator, then were returned to their home cages and housed for 1, 4, and 7 days.

2.4. Histochemical analysis of gene expression and infarct rim

After the designated survival periods, 13 adult and 12 aged rats were anesthetized with amobarbital (100 mg/kg i.p.) and perfused transcardially with 2% paraformaldehyde and 0.2% glutaraldehyde in PBS. The brain was removed and cut into coronal slices (3 mm thick) at the injected site and incubated in 5-bromo-4-chloro-3-indolyl-β-D-galactopyranoside (X-Gal, Wako Pure Chemical, Japan) staining solution for 3 h at room temperature. The slices of fixed brain were analyzed for positive staining in the macroscopic view, and sections (5 μm thick) were cut from the block with microtomes, placed on slides, and counterstained with hematoxyline-eosin for the identification of cells positively stained for β-galactosidase. The efficacy of transgene expression to the brain was assessed 1 day (adult and aged, $n = 4$ each), 4 days (adult and aged, $n = 4$ each), and 7 days (adult, $n = 5$; aged, $n = 4$) after injection of AdCMVβGal. Expression of β-galactosidase was analyzed semiquantitatively for the expression score, and scores were 0 (null), 1 (modest), 2 (moderate), or 3 (marked) as determined by a previously described method (Ooboshi et al., 2001). The rats that survived for 4 days were used for defining the mean distance of the infarct rim from the midline.

2.5. Biochemical assay for transgene

Seven days after brain ischemia was induced, gene transfer was quantitatively analyzed for the transgene expression in 4 adult and 5 aged SHR, as reported previously (Ooboshi et al., 1997). Briefly, the rats were perfused transcardially with ice-cold PBS, and each brain was removed. The coronal slice (2 mm thick) containing the injected site was cut from the brain block, and then 2-mm square cubes encompassing the injected sites (Fig. 2f) were assayed for β-galactosidase activity using an Aurola GAL-XE assay kit (Wako Pure Chemical, Japan). Light emission was measured with a luminometer, MiniLumat LB 9506 (Berthold, Germany), and was then calibrated with a standard curve generated with the use of purified *Escherichia coli* β-galactosidase (Boehringer Mannheim, Germany). Protein concentrations were determined using a Protein Assay CBB solution (Nacarai Tesque, Japan), and normalized β-galactosidase activity was expressed as mU β-galactosidase/mg protein.

2.6. Statistical analysis

Data are presented as the mean ± SEM. Differences in the data were analyzed by non-parametric Mann-Whitney *U*-test. $P < 0.05$ was regarded as statistically significant.

3. Results

3.1. Conditions at rest and during ischemia

The physiological parameters before and after ischemia in the adult and aged groups are shown in Table 1. No significant differences in the physiological variables between the two groups were seen, with the exception of MAP and hematocrit values. In addition, no significant differences were observed in the values obtained before and 1 h after distal MCA occlusion in each group. CBF at the occluded side began to decrease within 10 min after vessel occlusion, and changes in CBF were not significantly different between the aged and adult groups (Fig. 1). However, the infarct rim of the aged group tended to be closer to the midline (2.3 ± 0.2 mm) than that in adult group (2.7 ± 0.1, $P < 0.1$).

3.2. Transgene expression

Expression of the reporter gene (Fig. 2a) was consistently detected by histochemistry at C region. At I-p, transgene expression was detected 7 days after gene transfer in 3 of 5 adult rats and 3 of 4 aged rats. Positive staining for β-galactosidase at those regions was detected both in neurons and in non-neuronal cells (Fig. 2b and c). Transgene expression was observed both in the infarct area and in the non-infarct area at I-p (Fig. 2d). In the adult rats, there was no detectable expression at I-c. However, in the aged rats, transgene expression was observed at I-c (Fig. 2a), and the positive cells were mostly non-neuronal, e.g. astrocyte-like and endothelium-like cells (Fig. 2e). The time course of the semiquantitative analysis of transgene expression at each area is shown in Fig. 3. Transgene expression in the aged group at C was consistently detected from 1 to 7 days after gene transfer. However, expression of the reporter gene at I-p was not detected 1 day after the gene transfer, although it did begin to appear 4 days later. Similarly, transgene expression at I-c was not detected 1 day after the gene transfer and was only modestly present on day 4. These expression patterns in the aged group were similar to those in the adult group. However, the expression at I-c in adult rats disappeared 7 days after gene transfer (expression score 0; mean), whereas that in aged rats increased on day 7 (1.0, $P < 0.05$). The β-galactosidase activity at the injection site 7 days after gene transfer is shown in Fig. 4. The amount of expressed protein at I-c was significantly greater in the aged group than in the adult group (8 ± 4 mU/mg protein vs. 1 ± 1, $P < 0.05$), although that at C and I-p was similar in both groups.

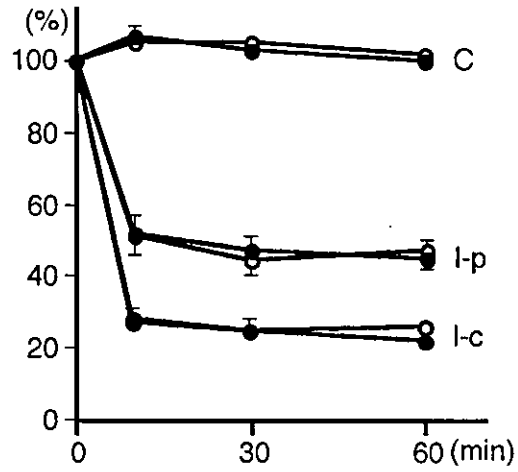

Fig. 1. Changes in cerebral blood flow at parietal cortices during distal middle cerebral artery occlusion. C, contralateral cortex. I-p, peri-ischemic area. I-c, ischemic core area. Aged group, closed circles. Adult group, open circles. Values are mean ± SEM. CBF, cerebral blood flow. dMCAO, distal middle cerebral artery occlusion.

Table 1
Physiological variables in adult and aged groups. (abbreviations: MAP, mean arterial pressure; dMCAO, distal middle cerebral artery occlusion)

At rest	Adult ($n = 17$)	Aged ($n = 17$)
MAP (mmHg)	192 ± 4	172 ± 6*
Rectal temperature (°C)	37.1 ± 0.0	37.1 ± 0.0
Head temperature (°C)	36.1 ± 0.0	36.1 ± 0.0
pH	7.41 ± 0.01	7.41 ± 0.01
PCO^2 (mmHg)	37.9 ± 0.8	39.0 ± 0.6
PO^2 (mmHg)	119 ± 4	107 ± 4
Hematocrit (%)	42 ± 0	40 ± 1#
Blood sugar (mmol/l)	8.9 ± 0.4	8.8 ± 0.3
1 h after dMCAO		
MAP (mmHg)	188 ± 4	174 ± 6#
Rectal temperature (°C)	37.1 ± 0.0	37.1 ± 0.0
Head temperature (°C)	36.1 ± 0.0	36.2 ± 0.0
pH	7.42 ± 0.01	7.42 ± 0.01
PCO2 (mmHg)	38.1 ± 0.8	37.8 ± 1.0
PO2 (mmHg)	125 ± 5	112 ± 6
Hematocrit (%)	43 ± 0	40 ± 1*
Blood sugar (mmol/l)	9.2 ± 0.5	8.8 ± 0.4

Values indicate means ± SEM. #$P < 0.05$, *$P < 0.01$ vs. adult group.

4. Discussion

The major new finding of the present study was that expression of the transgene in the ischemic core was greater in aged rats than that in adult rats 7 days after the induction of brain ischemia. Although transgene expression at the peri-ischemic area in aged rats was similar to that in adult rats, the infarct rim in aged rats tended to be closer to the midline than it was in the adult rats. These results suggest that adenovirus-mediated gene transfer to the ischemic brain may be more effective in the aged brain than in the adult brain.

Elderly populations are susceptible to ischemic stroke (Ueda et al., 1990). There are, however, few studies that examined the pathophysiology of brain ischemia using aged

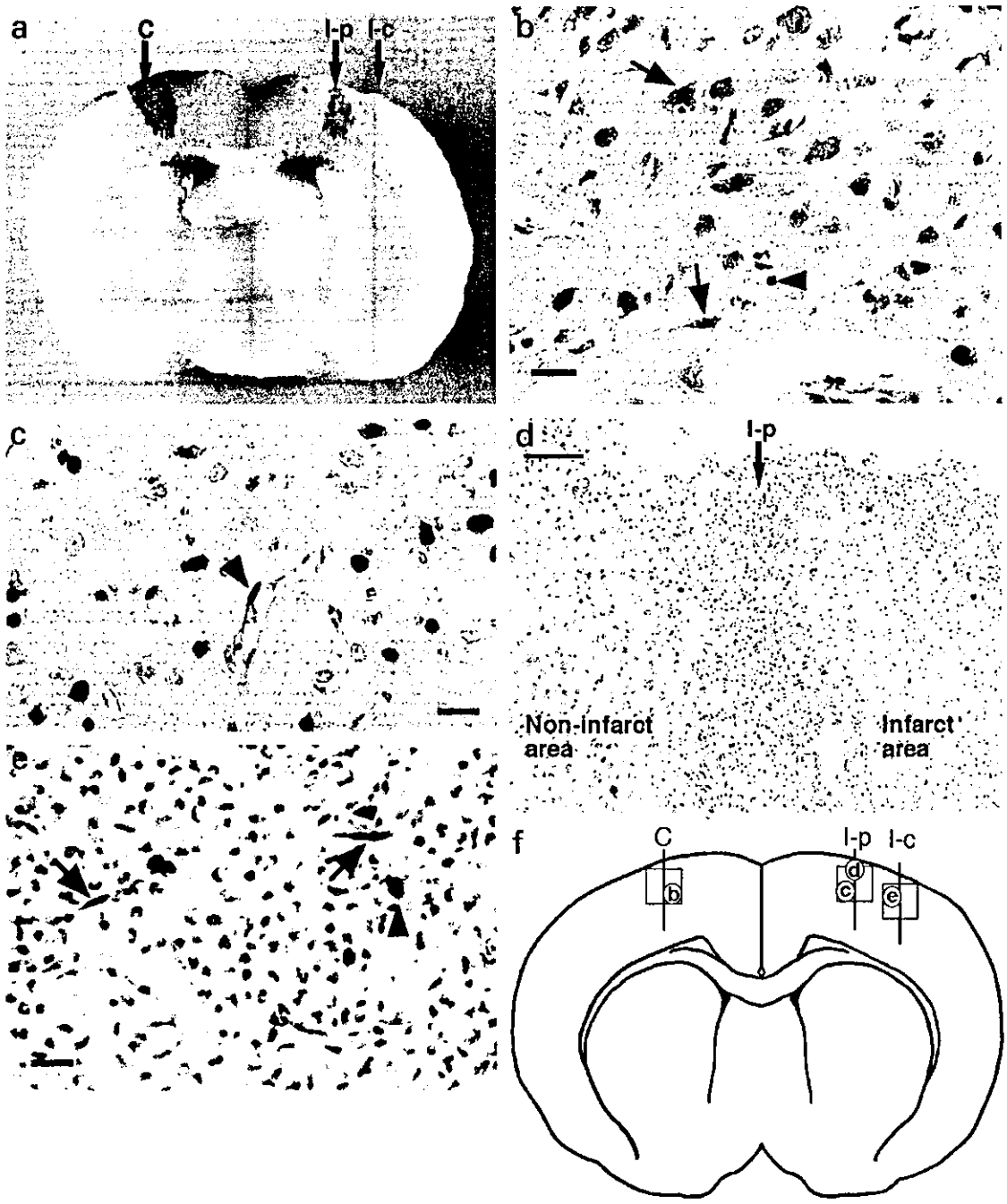

Fig. 2. Histochemical staining of the rat brain after the induction of brain ischemia and gene transfer. Expression of the reporter gene (β-galactosidase) detected in aged rats 7 days after the insult (a). Arrows indicate the areas of vector injection. C, contralateral cortex. I-p, peri-ischemic area. I-c, ischemic core area. In the microscopic view, positive staining for β-galactosidase was detected in aged rats (b–e). Neuron (b, arrows) and non-neuronal cells, including astrocyte-like (b, arrowhead) and endothelial (c, arrowhead) cells. Transgene expression at I-p region (d) and at I-c region (e). Non-neuronal cells, including astrocyte-like (e, arrowhead) and endothelium-like (e, arrows) cells. In f, circles indicate the location of b–e, respectively. Open squares indicate the location of tissues sampled for the biochemical assay. The bar represents 20 μm in b, c, and e, and 100 μm in d.

animals (Futrell et al., 1991; Davis et al., 1995). We previously showed that the ischemic damage to the striatum and hippocampus in aged rats was significantly greater than that observed in adult rats, although the reduction in CBF did not differ between the two groups (Yao et al., 1991). In another study, we also showed the protective effect of brain hypothermia in the aged rats (Ooboshi et al., 2000). Further studies using aged animals will be necessary for the clinical application of the specific treatments for brain ischemia. Moreover, studies of gene transfer to the ischemic brain in

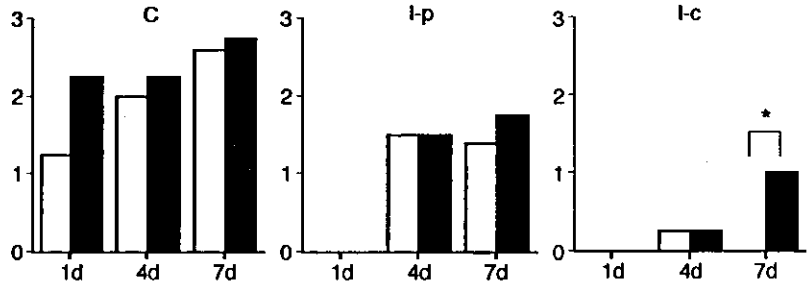

Fig. 3. The time course of transgene expression in the ischemic brain. Closed bars, aged group. Open bars, adult group. C, contralateral cortex. I-p, peri-ischemic area. I-c, ischemic core area. Bars represent the mean value. $*P < 0.05$.

aged models are very limited. Thus, the present study provides useful information for the investigation of the pathophysiology of brain ischemia in the aged populations.

In the present study, transgene expression was not detected in ischemic tissue 1 day after gene transfer in both adult and aged rats, whereas it was observed 4 days after gene transfer. A similar time course of the transgene expression was seen in another ischemic model (Abe et al., 1997). Previous reports have revealed that cerebral protein synthesis begins to decline when the CBF decreases to less than 50 % of the resting value (Xie et al., 1989; Mies et al., 1991). In our experiment, the average CBF at I-p and I-c was below the threshold value. Therefore, decreased protein synthesis in response to ischemia may lead to the delayed expression of the reporter gene. Whereas histochemical detection may underestimate the early expression of β-galactosidase (Zabner et al., 1994), the time course of postischemic transgene expression is an important therapeutic issue. Although most ischemic cell death occurs within 24 h after the onset of ischemia, delayed cell death also develops thereafter, even in cases of focal ischemia (Garcia et al., 1993; Du et al., 1996). Therefore, transgene expression, even at the subacute phase, would be useful for the treatment of brain ischemia.

Augmented transgene expression in aged animals is an interesting finding of this study. During the aging process, protein synthesis activity declines, and protein becomes inactivated by various types of protein modification (such as oxidation, glycation, or phosphorylation). By these means, protein turnover slows down (Rattan, 1996). Such changes would lead to decreased expression of the transgene. However, our present results demonstrated that transgene expression at I-c was augmented 7 days after gene transfer in the aged animals. Augmentation of expression might therefore be associated with the age-related decline of immune function, because inflammatory responses to adenovirus vector are major factors in the withdrawal of transgene expression (Lawrence et al., 1999), and such responses are attenuated in aged animals. Increased susceptibility of host cells to an adenoviral vector may be another mechanism of action. A previous study demonstrated that senescent cells expressed more αvβ5 integrins, known to be internalization receptors for adenoviruses, than did young cells (Hashimoto et al., 1997). Augmented expression of the adhesive factor in aged animals could promote transfection of the vector.

Previous reports demonstrated age-dependent enlargement of infarct volume following cerebral ischemia (Davis et al., 1994; Kharlamov et al., 2000). In our preliminary study, we used the same model as that used in the present study; it was found that the distance from the infarct rim to the midline in aged rats was significantly shorter than that in adult rats (unpublished data). In the present study, the infarct rim in aged rats also tended to be closer to the midline than that in adult rats, suggesting that the ischemia at I-p, which was located near the infarct rim, was more severe in the aged rats than that in the adult rats. However, transgene expression at I-p did not significantly differ between the two groups. Therefore, the transgene expression at

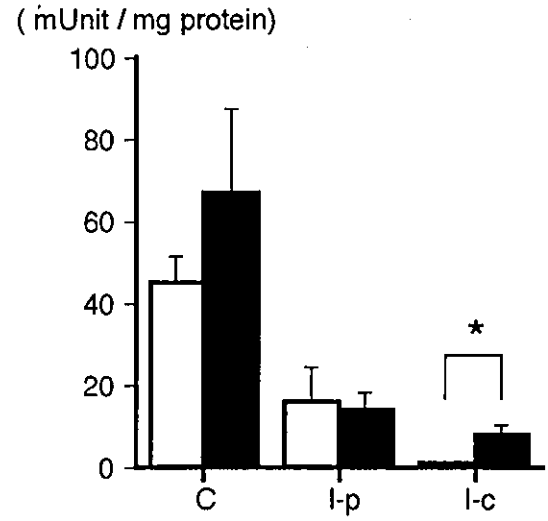

Fig. 4. Quantitative analysis of transgene expression at the parietal cortices 7 days after gene transfer. Closed bars, aged group. Open bars, adult group. C, contralateral cortex. I-p, peri-ischemic area. I-c, ischemic core area. Values are mean ± SEM. $*P < 0.05$.

the peri-ischemic area may be increased in aged than in adult rats.

In the present study, histological examination revealed that the cells which expressed β-galactosidase at I-c of aged rats were often round or spindle-shaped. The former cells appeared to be microglias and astrocytes, and the latter appeared to be endothelial cells. Brain ischemia induces the activation of resident microglial cells and blood-borne macrophages, the infiltration of leukocytes, and neuronal necrosis (Lehrmann et al., 1997; Schroeter et al., 1994, 1997). Such non-neuronal cells could also be potential targets for gene therapy, because transgene expression in these non-neuronal cells may improve cerebral blood flow, or facilitate tissue repair and neurogenesis in ischemic areas. In fact, a previous study demonstrated that interleukin-1 receptor antagonist, which was produced by transfected ependymal cells, reduced the infarct volume (Betz et al., 1995).

In conclusion, using an adenoviral vector encoding the β-galactosidase gene, we demonstrated coordinated or augmented transgene expression in the ischemic brain of aged rats, as compared with adult rats. The present results suggest that adenovirus-mediated gene transfer to the ischemic brain would provide effective transgene expression in aged rats. Brain ischemia in elderly populations may thus be a potential candidate for gene therapy.

Acknowledgements

This work was supported in part by the research grant in aid from the Ministry of Health and Welfare Comprehensive Research on Aging and Health (H11-008), Japan. We would like to thank the University of Iowa Gene Transfer Vector Core, especially Beverly L. Davidson and Richard D. Anderson, for viral vector preparations.

References

Abbott, A., 2001. Genetic medicine gets real. Nature 411, 410–412.

Abe, K., Setoguchi, Y., Hayashi, T., Itoyama, Y., 1997. In vivo adenovirus-mediated gene transfer and the expression in ischemic and reperfused rat brain. Brain Res. 763, 191–201.

Betz, A.L., Yang, G.Y., Davidson, B.L., 1995. Attenuation of stroke size in rats using an adenoviral vector to induce overexpression of interleukin-1 receptor antagonist in brain. J. Cereb. Blood Flow Metab. 15, 547–551.

Davidson, B.L., Allen, E.D., Kozarsky, K.F., Wilson, J.M., Roessler, B.J., 1993. A model system for in vivo gene transfer into the central nervous system using an adenoviral vector. Nat. Genet. 3, 219–223.

Davidson, B.L., Doran, S.E., Shewach, D.S., Latta, J.M., Hartman, J.W., Roessler, B.J., 1994. Expression of *Escherichia coli* β-galactosidase and rat HPRT in the CNS of *Macaca mulatta* following adenoviral mediated gene transfer. Exp. Neurol. 125, 258–267.

Davis, M., Mendelow, A.D., Perry, R.H., Chambers, I.R., James, O.F., 1994. The effect of age on cerebral oedema, cerebral infarction and neuroprotective potential in experimental occlusive stroke. Acta Neurochir. Suppl. 60, 282–284.

Davis, M., Mendelow, A.D., Perry, R.H., Chambers, I.R., James, O.F., 1995. Experimental stroke and neuroprotection in the aging rat brain. Stroke 26, 1072–1078.

Du, C., Hu, R., Csernansky, C.A., Hsu, C.Y., Choi, D.W., 1996. Very delayed infarction after mild focal cerebral ischemia: a role for apoptosis? J. Cereb. Blood Flow Metab. 16, 195–201.

Futrell, N., Garcia, J.H., Peterson, E., Millikan, C., 1991. Embolic stroke in aged rats. Stroke 22, 1582–1591.

Garcia, J.H., Yoshida, Y., Chen, H., Li, Y., Zhang, Z.G., Lian, J., Chen, S., Chopp, M., 1993. Progression from ischemic injury to infarct following middle cerebral artery occlusion in the rat. Am. J. Pathol. 142, 623–625.

Hashimoto, Y., Kohri, K., Akita, H., Mitani, K., Ikeda, K., Nakanishi, M., 1997. Efficient transfer of genes into senescent cells by adenovirus vectors via highly expressed αvβ5 integrin. Biochem. Biophys. Res. Commun. 240, 88–92.

Heistad, D.D., Faraci, F.M., 1996. Gene therapy for cerebral vascular disease. Stroke 27, 1688–1693.

Kharlamov, A., Kharlamov, E., Armstrong, D.M., 2000. Age-dependent increase in infarct volume following photochemically induced cerebral infarction: putative role of astroglia. J. Gerontol. A. Biol. Sci. Med. Sci. 55, B135–B141.

Lawrence, M.S., Foellmer, H.G., Elsworth, J.D., Kim, J.H., Leranth, C., Kozlowski, D.A., Bothwell, A.L.M., Davidson, B.L., Bohn, M.C., Redmond, D.E. Jr., 1999. Inflammatory responses and their impact on β-galactosidase transgene expression following adenovirus vector delivery to the primate caudate nucleus. Gene Ther. 6, 1368–1379.

Lehrmann, E., Christensen, T., Zimmer, J., Diemer, N.H., Finsen, B., 1997. Microglial and macrophage reactions mark progressive changes and define the penumbra in the rat neocortex and striatum after transient middle cerebral artery occlusion. J. Comp. Neurol. 386, 461–476.

Mies, G., Ishimaru, S., Xie, Y., Seo, K., Hossmann, K.A., 1991. Ischemic thresholds of cerebral protein synthesis and energy state following middle cerebral artery occlusion in rat. J. Cereb. Blood Flow Metab. 11, 735–761.

Millikan, C., 1992. Animal stroke models. Stroke 23, 795–797.

Ooboshi, H., Welsh, M.J., Rios, C.D., Davidson, B.L., Heistad, D.D., 1995a. Adenovirus-mediated gene transfer in vivo to cerebral blood vessels and perivascular tissue. Circ. Res. 77, 7–13.

Ooboshi, H., Sadoshima, S., Yao, H., Ibayashi, S., Matsumoto, T., Uchimura, H., Fujishima, M., 1995b. Ischemia-induced release of amino acids in the hippocampus of aged hypertensive rats. J. Cereb. Blood Flow Metab. 15, 227–234.

Ooboshi, H., Rios, C.D., Chu, Y., Christenson, S.D., Faraci, F.M., Davidson, B.L., Heistad, D.D., 1997. Augmented adenovirus-mediated gene transfer to atherosclerotic vessels. Arterioscler. Thromb. Vasc. Biol. 17, 1786–1792.

Ooboshi, H., Ibayashi, S., Takano, K., Sadoshima, S., Kondo, A., Uchimura, H., Fujishima, M., 2000. Hypothermia inhibits ischemia-induced efflux of amino acids and neuronal damage in the hippocampus of aged rats. Brain Res. 884, 23–30.

Ooboshi, H., Ibayashi, S., Takada, J., Yao, H., Kitazono, T., Fujishima, M., 2001. Adenovirus-mediated gene transfer to ischemic brain: ischemic flow threshold for transgene expression. Stroke 32, 1043–1047.

Rattan, S.I.S., 1996. Synthesis, modification, and turnover of proteins during aging. Exp. Gerontol. 31, 33–47.

Schroeter, M., Jander, S., Witte, O.W., Stoll, G., 1994. Local immune responses in the rat cerebral cortex after middle cerebral artery occlusion. J. Neuroimmunol. 55, 195–203.

Schroeter, M., Jander, S., Huitinga, I., Witte, O.W., Stoll, G., 1997. Phagocytic response in photochemically induced infarction of rat cerebral cortex: the role of resident microglia. Stroke 28, 383–386.

Ueda, K., Hasuo, Y., Ohmura, T., Kiyohara, Y., Kawano, H., Kato, I., Shinkawa, A., Iwamoto, H., Nakayama, K., Omae, T., Fujishima, M., 1990. Cause of death in the elderly and their changing pattern in Hisayama, a Japanese community. Results from a long-term and autopsy-based study. J. Am. Geriatr. Soc. 38, 1332–1338.

Xie, Y., Mies, G., Hossmann, K.A., 1989. Ischemic threshold of brain protein synthesis after unilateral carotid artery occlusion in gerbils. Stroke 20, 620–626.

Xu, D.G., Crocker, S.J., Doucet, J.P., St-Jean, M., Tamai, K., Hakim, A.M., Ikeda, J.E., Liston, P., Thompson, C.S., Korneluk, R.G., MacKenzie, A., Robertson, G.S., 1997. Elevation of neuronal expression of NAIP reduces ischemic damage in the rat hippocampus. Nat. Med. 3, 997–1004.

Yang, G.Y., Pang, L., Ge, H.L., Tan, M., Ye, W., Liu, X.H., Huang, F.P., Wu, D.C., Che, X.M., Song, Y., Wen, R., Sun, Y., 2001. Attenuation of ischemia-induced mouse brain injury by SAG, a redox-inducible antioxidant protein. J. Cereb. Blood Flow Metab. 21, 722–733.

Yao, H., Sadoshima, S., Ooboshi, H., Sato, Y., Uchimura, H., Fujishima, M., 1991. Age-related vulnerability to cerebral ischemia in spontaneously hypertensive rats. Stroke 22, 1414–1418.

Yao, H., Ibayashi, S., Sugimori, H., Fujii, K., Fujishima, M., 1996. Simplified model of krypton laser-induced thrombotic distal middle cerebral artery occlusion in spontaneously hypertensive rats. Stroke 27, 333–336.

Zabner, J., Couture, L.A., Smith, A.E., Welsh, M.J., 1994. Correction of cAMP-stimulated fluid secretion in cystic fibrosis airway epithelia: efficiency of adenovirus-mediated gene transfer in vitro. Hum. Gene Ther. 5, 585–593.

ATP-Sensitive Potassium Channels Mediate Dilatation of Basilar Artery in Response to Intracellular Acidification In Vivo

Naohiko Santa, MD; Takanari Kitazono, MD; Tetsuro Ago, MD; Hiroaki Ooboshi, MD; Masahiro Kamouchi, MD; Masanori Wakisaka, MD; Setsuro Ibayashi, MD; Mitsuo Iida, MD

Background and Purpose—During cerebral ischemia, both hypoxia and hypercapnia appear to produce marked dilatation of the cerebral arteries. Hypercapnia and hypoxia may be accompanied by extracellular and intracellular acidosis, which is another potent dilator of cerebral arteries. However, the precise mechanism by which acidosis produces dilatation of the cerebral arteries is not fully understood. The objective of the present study was to examine the mechanisms by which intracellular acidosis produces dilatation of the basilar artery in vivo.

Methods—Using a cranial window in anesthetized rats, we examined responses of the basilar artery to sodium propionate, which was used to cause intracellular acidosis specifically. Expression of subunits of potassium channels was determined by reverse transcription and polymerase chain reaction (RT-PCR).

Results—Topical application of propionate increased diameter of the basilar artery in a concentration-related manner. Propionate-induced dilatation of the artery was attenuated by glibenclamide, an inhibitor of ATP-sensitive potassium channels. However, inhibitors of nitric oxide synthase (N^G-nitro-L-arginine), large-conductance calcium-activated potassium channels (iberiotoxin), and cyclooxygenase (indomethacin) did not affect the vasodilatation. Expression of mRNA for SUR2B and Kir6.1 was detected, with the use of RT-PCR, in the cultured basilar arterial muscle cells.

Conclusions—The findings suggest that intracellular acidification may produce dilatation of the basilar artery through activation of ATP-sensitive potassium channels in vivo. Kir6.1/SUR2B may be the major potassium channels that mediate propionate-induced dilatation of the artery. (***Stroke.* 2003;34:1276-1280.)**

Key Words: muscle, smooth ■ propionic acids ■ vasodilation

During cerebral ischemia, both hypoxia and hypercapnia appear to produce marked dilatation of the cerebral arteries.[1] The vasodilator responses may increase cerebral perfusion for maintenance of oxygen delivery to brain tissue. Both hypoxia and hypercapnia may be accompanied by extracellular and/or intracellular acidosis. Recent evidence has suggested that acidosis itself produces marked relaxation of the cerebral arteries in vitro.[2,3] Thus, extracellular and intracellular acidosis may play a major role in dilatation of the cerebral arteries during hypoxia and hypercapnia.[4]

Hypoxic dilatation of the cerebral arteries appears to be mediated by activation of ATP-sensitive potassium (K_{ATP}) channels.[5,6] On the other hand, vasodilatation induced by hypercapnia is reported to be mediated mainly by nitric oxide (NO).[7,8] Thus, the mechanisms by which acidosis produces dilatation of the cerebral arteries may be quite different between hypoxia and hypercapnia. It is reported that extracellular pH (pH_o) rather than intracellular pH (pH_i) may be the major determinant of hypercapnia-induced, NO-dependent relaxation of the cerebral arteries in vitro.[3] Hypoxia appears to produce dilatation of the cerebral arterioles through activation of K_{ATP} channels that is independent of pH_o changes,[4] suggesting that pH_o may not be important in hypoxia-induced activation of K_{ATP} channels in cerebrovascular muscle.

Recently, Xu et al[9] showed that K_{ATP} channels expressed in *Xenopus* oocytes are activated directly by intracellular but not extracellular acidosis. The findings suggest that K_{ATP} channels contain their pH-sensitive sites in the inside of the cell membrane. However, it is not known whether selective intracellular acidosis activates K_{ATP} channels and thereby produces dilatation of the cerebral arteries in vivo. Thus, the first objective of the present study was to test the hypothesis that intracellular acidosis of the basilar arterial muscle cells produces dilatation of the artery through activation of K_{ATP} channels in vivo.

The activity of K_{ATP} channels has been shown in cerebrovascular muscle and appears to play an important role in dilator responses of the cerebral arteries.[5,6,10,11] It has been shown that K_{ATP} channels are hetero-octamers consisting of 4 sulfonylurea receptors (SUR) interacting with 4 channel subunits (Kir channels).[12,13] SUR2B may be the major SUR in the smooth muscle cells of systemic arteries.[14] Both Kir6.1 and Kir6.2 are reported to be present in vascular muscle

Received August 7, 2002; final revision received October 25, 2002; accepted December 2, 2002.

From the Department of Medicine and Clinical Science, Graduate School of Medical Sciences, Kyushu University, Fukuoka, Japan.

Correspondence to Takanari Kitazono, MD, PhD, Department of Medicine and Clinical Science, Graduate School of Medical Sciences, Kyushu University, Maidashi 3-1-1, Higashi-ku, Fukuoka 812-8582, Japan. E-mail kitazono@intmed2.med.kyushu-u.ac.jp

***Stroke* is available at http://www.strokeaha.org** **DOI: 10.1161/01.STR.0000068171.01248.97**

cells.[9,15,16] However, it is not known which Kir is expressed in the cerebral arterial muscle. Thus, the second objective was to determine SUR and Kir subunits expressed in the basilar arterial muscle cells.

Materials and Methods

This experiment was reviewed by the Committee on the Ethics of Animal Experiments in the Faculty of Medicine, Kyushu University, and performed under the control of the Guidelines for Animal Experiments in the Faculty of Medicine, Kyushu University, and the Law (No. 105) and Notification (No. 6) of the Japanese government.

Cranial Window

Experiments were performed on male Sprague-Dawley rats (weight, 400±8 g; age, 3.4±0.2 months [mean±SEM]) anesthetized with amobarbital (100 mg/kg IP). Anesthesia was supplemented intravenously at 20 to 25 mg/kg per hour. The trachea was cannulated, and the animals were mechanically ventilated with room air and supplemental oxygen. Skeletal muscle paralysis was produced with *d*-tubocurarine chloride (2 mg/kg). Depth of anesthesia was evaluated by applying pressure to a paw or the tail and observing changes in heart rate or blood pressure. When such changes occurred, additional anesthetic was administered. Catheters were placed in both femoral arteries to measure systemic arterial pressure and to obtain arterial blood samples. A femoral vein was cannulated for infusion of drugs.

A craniotomy was prepared over the ventral brain stem as previously described in detail.[17] After a part of the dura was opened, the cranial window was suffused with artificial cerebrospinal fluid (CSF) (temperature=37°C; ionic composition [in mmol/L]: 132 NaCl, 2.95 KCl, 1.71 $CaCl_2$, 0.65 $MgCl_2$, 24.6 $NaHCO_3$, 3.69 D-glucose) that was bubbled continuously with appropriate gases. The diameter of the blood vessel was measured with the use of a microscope equipped with a television camera coupled to an auto-width analyzer (C3161, Hamamatsu Photonics KK). After craniotomy was performed, pH, P_{CO_2}, and P_{O_2} of arterial blood were adjusted by changing rate and volume of the respirator and the oxygen content of inspiratory air. We also monitored arterial blood gas during the experiments and kept the values within normal limits (pH=7.45±0.01, P_{CO_2}=39±1 mm Hg, and P_{O_2}=93±4 mm Hg).

We examined responses of the basilar artery to topical application of sodium propionate (10^{-6} to 10^{-3} mol/L). Sodium propionate permeates the cells in its protonated form and releases protons, which produces intracellular acidification.[18] We also examined responses to sodium nitroprusside (10^{-8} to 10^{-6} mol/L), an NO donor. Each drug was mixed in artificial CSF and suffused over the craniotomy for 5 minutes. Diameters of the basilar artery were measured immediately before and during the last minute of application of each agonist. After application of a specific drug, the vessel diameter returned to baseline level within a few minutes before application of another one. The application sequence was alternative. We also examined pH, P_{CO_2}, and P_{O_2} of artificial CSF in the absence and presence of 1 mmol/L sodium propionate. Application of the concentration of propionate did not affect these parameters of the CSF (control: pH=7.43±0.02, P_{CO_2}=35±1 mm Hg, and P_{O_2}=119±3 mm Hg; propionate: pH=7.42±0.02, P_{CO_2}=35±1 mm Hg, and P_{O_2}=119±3 mm Hg; n=10).

We used glibenclamide (10^{-6} mol/L), an inhibitor of K_{ATP} channels,[6] N^G-nitro-L-arginine (L-NNA) (10^{-5} mol/L), an inhibitor of NO synthase,[19] iberiotoxin (10^{-5} mol/L), an inhibitor of large conductance calcium-activated potassium channels,[6,20] and indomethacin (10 mg/kg IV), an inhibitor of cyclooxygenase.[21] Each inhibitor appears to produce maximum inhibition of its target molecule at the concentration described above.[6,19–21] Glibenclamide was dissolved in dimethyl sulfoxide (DMSO). The maximum final concentration of DMSO was 0.1%. We found that 0.1% DMSO did not cause any significant changes in diameter of the basilar artery (1±2%; n=5). Other inhibitors were dissolved in distilled water. L-NNA was suffused starting from 15 minutes before and during application of propionate or nitroprusside. Suffusion of other inhibitors was started from 5 minutes before application of sodium propionate or sodium nitroprusside. Topical application of these agents did not cause any changes in systemic arterial pressure.

To confirm the importance of pH_i changes in propionate-induced vasodilatation, we tested the effects of 5-*N*,*N*-hexamethyleneamiloride, an inhibitor of Na^+/H^+ exchanger,[18,22,23] on the vasodilatation. 5-*N*,*N*-Hexamethyleneamiloride (3 μmol/L) was dissolved in DMSO and suffused 5 minutes before and during application of sodium propionate or sodium nitroprusside. The final concentration of DMSO in the CSF was 0.1%.

TABLE 1. Nucleotide Sequences of Primers Used for PCR and Expected Size of PCR Products

mRNA	Expected Size	Primer Sequence (5′→3′)
rKir6.1	1275	Forward-ATGCTGGCCAGGAAGAGCAT
		Reverse-TCATGATTCTGATGGGCACT
rKir6.2	1173	Forward-ATGCTGTCCCGAAAAGGCAT
		Reverse-TCAGGACAAGGAATCCGGAG
rSUR2B	858	Forward-GTTGTAAGGAACTTGGCCGA
		Reverse-TCACATGTCCGCACGAACGA

Reverse Transcription and Polymerase Chain Reaction

Basilar arterial muscle cells were collected from the basilar artery of male Sprague-Dawley rats (aged 4 to 6 weeks).[24] After they were anesthetized with diethyl ether, the animals were decapitated, and the basilar artery was quickly removed under sterile conditions. The arterial segments were carefully cleaned of connective tissue, cut into small fragments, and placed in culture dishes coated with collagen type 1. The growth medium (Dulbecco's modified Eagle's medium) was supplemented with 10% fetal bovine serum and 1% penicillin-streptomycin solution. The dishes were incubated at 37°C in a humidified atmosphere of 95% air and 5% CO_2. After a few days, colonies of vascular muscle cells proliferated from the basilar arterial segments. After the arterial segment was removed, the primary vascular muscle cell colonies were gently scraped off and subcultured in other dishes. Final characterization of the cells was performed by demonstrating the absence of di-I LDL uptake and the expression of smooth muscle–specific α-actin.

Total RNA was prepared from cultured basilar arterial muscle cells with TRIzol reagent (Life technologies, Inc).[25] With the use of 1 μg total RNA, first strand cDNA synthesis was performed by AMV transcriptase in 20 μL (Roche Diagnostics). With the use of aliquots (1 μL) of reverse transcriptase (RT) products, polymerase chain reaction (PCR) reactions were performed in 50 μL final volumes with the gene-specific primers listed in Table 1. Amplification was performed for 30 cycles of denaturation at 94°C (30 seconds), annealing at 60°C (30 seconds), and extension at 72°C (60 seconds), followed by 7 minutes of extension reaction at 72°C. PCR products were separated on 1% agarose gel.

We also examined the expression of K_{ATP} channels in pancreatic cells. After they were anesthetized with diethyl ether, male Sprague-Dawley rats (aged 6 weeks) were decapitated, and the pancreas was quickly removed. The organ was dispersed with a dispersing generator (POLYTRON PT2100, Kinematica AG), and total RNA was prepared with TRIzol reagent. RT-PCR was performed as described above.

Statistical Analysis

All values were expressed as mean±SEM. One-way repeated-measures ANOVA was used to compare concentration-dependent responses to vasodilators. Two-way repeated-measures ANOVA was used to compare responses under control conditions and during interventions. When a significant F value was found, post hoc analysis was performed with the Wilcoxon test. A value of $P<0.05$ was considered significant.

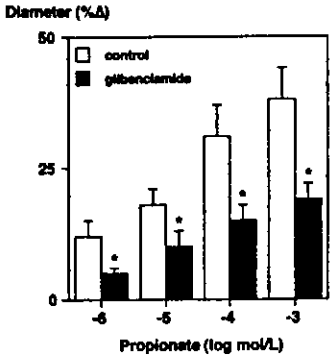

Figure 1. Effects of glibenclamide on propionate-induced vasodilatation. Changes in diameter of the basilar artery were measured in response to sodium propionate (10^{-6} to 10^{-3} mol/L) under control conditions and in the presence of glibenclamide (10^{-6} mol/L). Values are mean±SEM; n=6. *P<0.05 vs control response.

Results

Propionate-Induced Vasodilatation

Under control conditions, diameter of the basilar artery was 224±7 μm (n=20). Topical application of sodium propionate (10^{-6} to 10^{-3} mol/L) produced dilatation of the basilar artery in a concentration-related manner (Figure 1). Vasodilatation induced by propionate (10^{-6} to 10^{-3} mol/L) was reproducible since there was no significant attenuation of the response during repeated application of propionate (first: 11±2%, 19±3%, 28±5%, 36±6%, respectively; second: 10±2%, 19±4%, 29±6%, 34±5%, respectively; n=5). Glibenclamide, a selective inhibitor of K_{ATP} channels, had no effects on the baseline diameter of the basilar artery but inhibited dilatation of the basilar artery in response to propionate (Figure 1). We found that 10^{-6} mol/L glibenclamide inhibited vasodilatation in response to 10^{-3} mol/L sodium propionate by 46±11%. Sodium nitroprusside (10^{-8} to 10^{-6} mol/L) also produced dilatation of the basilar artery (Figure 2). Glibenclamide (10^{-6} mol/L) did not affect vasodilatation produced by sodium nitroprusside (Figure 2). We also tested the effects of L-NNA (10^{-5} mol/L), iberiotoxin (10^{-5} mol/L), and indomethacin (10 mg/kg IV) on propionate-induced dilatation of the basilar artery. None of the inhibitors affected propionate-induced vasodilatation (Table 2).

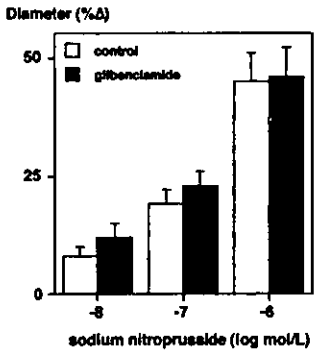

Figure 2. Effects of glibenclamide on nitroprusside-induced vasodilatation. Changes in diameter of the basilar artery were measured in response to sodium nitroprusside (10^{-8} to 10^{-6} mol/L) under control conditions and in the presence of glibenclamide (10^{-6} mol/L). Values are mean±SEM; n=6.

TABLE 2. Effects of Inhibitors on Propionate-Induced Vasodilatation

	Vasodilatation, %			
Propionate, mol/L	Control (n=7)	Iberiotoxin (n=5)	Indomethacin (n=5)	L-NNA (n=5)
10^{-6}	12±3	11±2	12±4	11±3
10^{-5}	18±3	20±4	20±4	17±4
10^{-4}	31±6	27±4	28±4	23±3
10^{-3}	38±6	35±5	36±4	38±4

Because intracellular acidification activates the Na^+/H^+ exchanger, which causes efflux of protons to the extracellular space and thereby normalizes intracellular pH,[18,26] inhibition of the Na^+/H^+ exchanger enhances intracellular acidification.[26] Thus, we anticipated that inhibition of the exchanger would enhance propionate-induced vasodilatation. In the present study 5-*N*,*N*-hexamethyleneamiloride (3 μmol/L), an inhibitor of Na^+/H^+ exchanger, enhanced propionate-induced dilatation of the basilar artery (Figure 3); 3 μmol/L 5-*N*,*N*-hexamethyleneamiloride did not affect vasodilator responses to sodium nitroprusside (10^{-8} to 10^{-6} mol/L). The findings suggest that propionate-induced vasodilatation is dependent on intracellular acidification.

Presence of Kir6.1 and SUR2B

RT-PCR reactions yielded an expected-size 1275-bp PCR product for Kir6.1 but not an expected-size 1173-bp product for Kir6.2 (Figure 4), indicating that the vascular smooth muscle cells mainly expressed Kir6.1. Identical results were obtained with several independent vascular muscle isolates. On the other hand, pancreatic cells expressed Kir6.2 but not Kir6.1 (Figure 4). We also tested whether the vascular cells expressed SUR2B, which is reported to be present in rat coronary arterial muscle cells. RT-PCR reactions yielded an expected-size 858-bp PCR product for SUR2B (Figure 4).

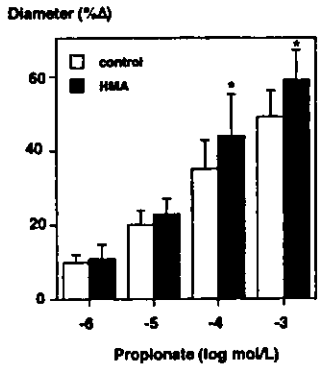

Figure 3. Effects of 5-*N*,*N*-hexamethyleneamiloride (HMA) on propionate-induced vasodilatation. Changes in diameter of the basilar artery were measured in response to sodium propionate (10^{-6} to 10^{-3} mol/L) under control conditions and in the presence of 5-*N*,*N*-hexamethyleneamiloride (3×10^{-6} mol/L). Values are mean±SEM; n=6. *P<0.05 vs control response.

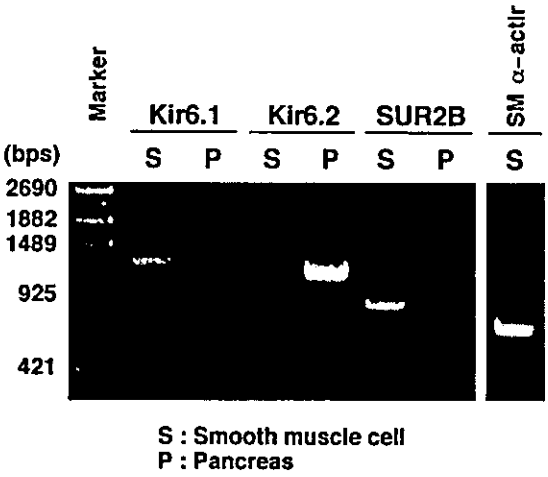

Figure 4. Presence of Kir6.1 and SUR2B. RT-PCR reactions yielded an expected-size 1275-bp PCR product for Kir6.1 but not an expected-size 1173-bp product for Kir6.2 in cultured basilar arterial muscle cells. RT-PCR reactions also yielded an expected-size 858-bp PCR product for SUR2B. Identical results were obtained with several independent vascular muscle isolates. SM indicates smooth muscle.

Discussion

There are 2 major new findings in the present study. First, intracellular acidosis of vascular muscle by sodium propionate produced marked dilatation of the basilar artery, and the vasodilatation may be mediated, at least in part, by activation of K_{ATP} channels in vivo. Second, Kir6.1 but not Kir6.2 was expressed in the basilar arterial muscle cells. Because SUR2B was also expressed in the muscle cells, Kir6.1/SUR2B may be the major K_{ATP} channels that mediate propionate-induced dilatation of the basilar artery.

During cerebral ischemia, dilatation of the cerebral arteries appears to occur.[1] The mechanisms of ischemia-induced vasodilatation are very complicated.[1] Several factors, including hypoxia and hypercapnia, may account for ischemia-induced vasodilatation. Because both hypoxia and hypercapnia may be accompanied by intracellular and extracellular acidosis and acidosis itself produces marked dilatation of the cerebral arteries,[2,3] decrease of pH_o and pH_i may play an important role in dilatation of the cerebral arteries during hypoxia and hypercapnia. In the present study we focused on intracellular acidosis because that may be the first phenomenon that occurs after ischemic insult. Sodium propionate appears to decrease pH_i without affecting pH_o.[18] We also showed that propionate did not affect pH_o, Pco_2, or Po_2 in the artificial CSF. Because propionate caused marked dilatation of the basilar artery, intracellular acidosis of vascular muscle itself may produce dilatation of the artery in vivo. Moreover, 5-*N*,*N*-hexamethyleneamiloride enhanced dilatation of the basilar artery in response to sodium propionate. The findings may also support the interpretation that propionate-induced dilatation of the basilar artery may be mediated by intracellular acidification in vivo.

To examine the role of K_{ATP} channels in propionate-induced dilatation of the basilar artery, we tested effects of glibenclamide, an inhibitor of K_{ATP} channels,[6] on the vasodilatation. Glibenclamide inhibited propionate-induced dilatation of the artery by approximately 50%. Thus, dilatation of the artery in response to intracellular acidosis may be mediated, in large part, by activation of K_{ATP} channels in vivo. The findings are similar to those of Ishizaka and Kuo[27] that acidosis-induced relaxation of porcine coronary artery is mediated primarily by activation of K_{ATP} channels in vitro. The mechanisms of acidosis-induced activation of K_{ATP} channels are still unclear. Ishizaka and Kuo[27] have suggested that acidosis produces activation of pertussis toxin–sensitive GTP-binding protein and thereby causes vasorelaxation. Recently, Xu et al,[9] using a patch-clamp technique, showed that protons activate the intracellular domain of K_{ATP} channels and increase the open probability of the channels. Thus, it may be possible that selective intracellular acidification activates K_{ATP} channels of basilar arterial muscle cells and thereby causes dilatation of the artery.

We also tested the effects of 3 other inhibitors, ie, L-NNA, iberiotoxin, and indomethacin. However, none of these inhibitors affected propionate-induced dilatation of the basilar artery. Thus, NO, BK_{Ca} channels, and prostanoids may not be involved in propionate-induced dilatation of the basilar artery in vivo. Horiuchi et al[28] examined responses of the cerebral arteries in response to extracellular acidification by HCl and showed that both NO and K_{ATP} channels are involved in acidosis-induced relaxation of the arteries in vitro. pH_o instead of pH_i appears to be the major determinant of hypercapnia-induced, NO-dependent relaxation of the cerebral arteries in vitro.[3] Thus, it may be possible that application of HCl to the vascular muscle reduced pH_o as well as pH_i and thereby activated both NO production and K_{ATP} channels of the cerebral arterioles.

Glibenclamide at the concentration of 10^{-5} mol/L reduced but did not abolish propionate-induced dilatation of the basilar artery. Several mechanisms may be involved in the residual vasodilatation. It is reported that normocapnic acidosis inhibited calcium influx without affecting membrane potential of vascular muscle cells.[29] Thus, acidosis may also inhibit calcium channels in the vascular muscle independent of the activity of potassium channels, and the residual vasodilatation after inhibition of K_{ATP} channels is mediated by such direct inhibitory actions of acidosis on calcium channels. The activity of inward rectifier potassium channels is reported to be modulated by acidosis.[30,31] Thus, we cannot exclude the possibility that inward rectifier potassium channels may be involved in the residual dilatation of the basilar artery. We also cannot exclude the possibility that other unknown mechanisms are involved in propionate-induced dilatation of the basilar artery in vivo.

K_{ATP} channels are hetero-octamers consisting of 4 sulfonylurea receptors (SUR) interacting with 4 channel subunits (Kir channels). SUR2B appears to represent the SUR in the vascular muscle type K_{ATP} channels. We also found that SUR2B was expressed in the basilar arterial muscle cells. On the other hand, both Kir6.1 and Kir6.2 are reported to be present in vascular muscle cells. Isomoto et al[15] showed that coexpression of Kir6.2 and SUR2B reconstitutes the pharmacological and electrophysiological properties of K_{ATP} channels described in smooth muscle cells. However, Yamada et

al[32] suggested that K^+ channels composed of Kir6.1 and SUR2B closely resemble K_{ATP} channels observed in vascular muscle cells. In the present study we found that Kir6.1 is expressed in the basilar arterial muscle cells; however, significant expression of Kir6.2 was not observed in the muscle cells. Thus, Kir6.1/SUR2B may be the major K_{ATP} channels in the basilar arterial muscle cells. Xu et al[9] showed that protons act directly on the Kir6 subunits and thereby increase channel activity. Thus, dilatation of the basilar artery in response to intracellular acidosis may be produced by activation of Kir6.1/SUR2B channels in the basilar arterial muscle cells by protons. However, we cannot exclude the possibility that the pattern of expression of the channels in cultured muscle cells is different from that in intact cells.

In conclusion, sodium propionate produced dilatation of the basilar artery in vivo. Propionate-induced vasodilatation may be due to intracellular acidification of the basilar arterial muscle cells and may be mediated in part by activation of K_{ATP} channels. Kir6.1/SUR2B may be the major K_{ATP} channels in the basilar arterial muscle cells.

Acknowledgments

This study was supported in part by a research grant for cardiovascular diseases (11C-1) from the Ministry of Health and Welfare, Japan. A part of this study was performed in the Kyushu University Station for Collaborative Research.

References

1. Iadecola C. Cerebral circulatory dysregulation in ischemia. In: Ginsberg MD, Bogousslavsky J, eds. *Cerebrovascular Disease: Pathophysiology, Diagnosis, and Management*. Malden, Mass: Blackwell Science; 1998: 319–332.
2. Dietrich HH, Dacey RG Jr. Effects of extravascular acidification and extravascular alkalinization on constriction and depolarization in rat cerebral arterioles in vitro. *J Neurosurg*. 1994;81:437–442.
3. Tian R, Vogel P, Lassen NA, Mulvany MJ, Andreasen F, Aalkjaer C. Role of extracellular and intracellular acidosis for hypercapnia-induced inhibition of tension of isolated rat cerebral arteries. *Circ Res*. 1995;76: 269–275.
4. Aalkjaer C, Peng HL. pH and smooth muscle. *Acta Physiol Scand*. 1997;161:557–566.
5. Taguchi H, Heistad DD, Kitazono T, Faraci FM. ATP-sensitive K^+ channels mediate dilatation of cerebral arterioles during hypoxia. *Circ Res*. 1994;74:1005–1008.
6. Kitazono T, Faraci FM, Taguchi H, Heistad DD. Role of potassium channels in cerebral blood vessels. *Stroke*. 1995;26:1713–1723.
7. Faraci FM, Breese KR, Heistad DD. Cerebral vasodilation during hypercapnia: role of glibenclamide-sensitive potassium channels and nitric oxide. *Stroke*. 1994;25:1679–1683.
8. Faraci FM, Brian JE Jr. Nitric oxide and the cerebral circulation. *Stroke*. 1994;25:692–703.
9. Xu H, Cui N, Yang Z, Wu J, Giwa LR, Abdulkadir L, Sharma P, Jiang C. Direct activation of cloned K_{ATP} channels by intracellular acidosis. *J Biol Chem*. 2001;276:12898–12902.
10. Kitazono T, Faraci FM, Heistad DD. Effect of norepinephrine on rat basilar artery in vivo. *Am J Physiol*. 1993;264:H178–H182.
11. Kitazono T, Heistad DD, Faraci FM. Role of ATP-sensitive K^+ channels in CGRP-induced dilatation of basilar artery in vivo. *Am J Physiol*. 1993;265:H581–H585.
12. Aschcroft FM, Gribble FM. Correlating structure and function in ATP-sensitive K^+ channels. *Trends Neurosci*. 1998;21:288–294.
13. Fujita A, Kurachi Y. Molecular aspects of ATP-sensitive K^+ channels in the cardiovascular system and K^+ channel openers. *Pharmacol Ther*. 2000;85:39–53.
14. Davis-Taber R, Choi W, Feng JL, Hoogenboom L, McNally T, Kroeger P, Shieh CC, Simmer R, Brioni JD, Sullivan JP, Gopalakrishnan M, Scott VES. Molecular characterization of human SUR2-containing K_{ATP} channels. *Gene*. 2000;256:261–270.
15. Isomoto S, Kondo C, Yamada M, Matsumoto S, Higashiguchi O, Horio Y, Matsuzawa Y, Kurachi Y. A novel sulfonylurea receptor forms with BIR (Kir6.2) a smooth muscle type ATP-sensitive K^+ channel. *J Biol Chem*. 1996;271:24321–24324.
16. Suzuki M, Li RA, Miki T, Uemura H, Sakamoto N, Ohmoto-Sekine Y, Tamagawa M, Ogura T, Seino S, Marban E, Nakaya H. Functional roles of cardiac and vascular ATP-sensitive potassium channels clarified by Kir6.2-knockout mice. *Circ Res*. 2001;88:570–577.
17. Faraci FM, Heistad DD, Mayhan WG. Role of large arteries in regulation of blood flow to brain stem in cats. *J Physiol*. 1987;387:15–23.
18. Kitazono T, Takeshige K, Cragoe EJ Jr, Minakami S. Intracellular pH changes of cultured bovine aortic endothelial cells in response to ATP addition. *Biochem Biophys Res Commun*. 1988;152:1304–1309.
19. Moncada S, Palmer RMJ, Higgs EA. Nitric oxide: physiology, pathophysiology, and pharmacology. *Pharmacol Rev*. 1991;43:109–142.
20. Kitazono T, Ibayashi S, Nagao T, Fujii K, Fujishima M. Role of Ca^{2+}-activated K^+ channels in acetylcholine-induced dilatation of the basilar artery in vivo. *Br J Pharamacol*. 1997;120:102–106.
21. Faraci FM, Sobey CG, Chrissobolis S, Lund DD, Heistad DD, Weintraub NL. Arachidonate dilates basilar artery by lipoxygenase-dependent mechanism and activation of K^+ channels. *Am J Physiol*. 2001;281: R246–R253.
22. Kleyman TR, Cragoe EJ Jr. Amiloride and its analogs as tools in the study of ion transport. *J Membr Biol*. 1988;105:1–21.
23. Kitazono T, Takeshige K, Cragoe EJ Jr, Minakami S. Involvement of calcium and protein kinase C in the activation of the Na^+/H^+ exchanger in cultured bovine aortic endothelial cells stimulated by extracellular ATP. *Biochim Biophys Acta*. 1989;1013:152–158.
24. Kitayama J, Kitazono T, Ibayashi S, Wakisaka M, Watanabe Y, Kamouchi M, Nagao T, Fujishima M. Role of phosphatidylinositol 3-kinase in acetylcholine-induced dilatation of rat basilar artery. *Stroke*. 2000;31:2487–2493.
25. Ago T, Nunoi H, Ito T, Sumimoto H. Mechanism for phosphorylation-induced activation of the phagocyte NADPH oxidase protein p47phox: triple replacement of serine 303, 304, 328 with aspartates disrupts the SH3 domain-mediated intramolecular interaction in p47phox, thereby activating the oxidase. *J Biol Chem*. 1999;274:33644–33653.
26. Putney LK, Denker SP, Barber DL. The changing face of the Na^+/H^+ exchanger, NHE1: structure, regulation, and cellular actions. *Annu Rev Pharmacol Toxicol*. 2002;42:527–552.
27. Ishizaka H, Kuo L. Acidosis-induced coronary arteriolar dilation is mediated by ATP-sensitive potassium channels in vascular smooth muscle. *Circ Res*. 1996;78:50–57.
28. Horiuchi T, Dietrich HH, Hongo K, Goto T, Dacey RG Jr. Role of endothelial nitric oxide and smooth muscle potassium channels in cerebral arteriolar dilation in response to acidosis. *Stroke*. 2002;33: 844–849.
29. Peng H-L, Jensen PE, Nilsson H, Aalkjaer C. Effect of acidosis on tension and $[Ca^{2+}]_i$ in rat cerebral arteries: is there a role for membrane potential? *Am J Physiol*. 1998;274:H655–H662.
30. Ito H, Vereecke J, Carmeliet E. Intracellular protons inhibit inward rectifier K^+ channels of guinea-pig ventricular cell membrane. *Pflugers Arch*. 1992;422:280–286.
31. Xu H, Cui N, Yang Z, Qu Z, Jiang C. Modulation of Kir4.1 and Kir5.1 by hypercapnia and intracellular acidosis. *J Physiol*. 2000;524:725–735.
32. Yamada K, Ji JJ, Yuan H, Miki T, Sato S, Horimoto N, Shimizu T, Seino S, Inagaki N. Protective role of ATP-sensitive potassium channels in hypoxia-induced generalized seizure. *Science*. 2001;292:1543–1546.

Reprinted from JOURNAL OF NEUROLOGY, NEUROSURGERY & PSYCHIATRY, May 2003, Vol 74, No 5, p 649-653

SHORT REPORT

Reappraisal of early CT signs to predict the arterial occlusion site in acute embolic stroke

M Koga, Y Saku, K Toyoda, H Takaba, S Ibayashi, M Iida

J Neurol Neurosurg Psychiatry 2003;74:649–653

Objective: To elucidate the value of early computed tomographic (CT) signs of stroke in predicting the occlusion site in the cerebral arteries.
Patients: 105 consecutive patients with acute embolic stroke affecting the anterior circulation.
Methods: Four early signs were evaluated on cranial CT within six hours of stroke onset: loss of the insular ribbon (LIR); attenuation of the lentiform nucleus (ALN); hemispherical sulcus effacement (HSE); and the hyperdense middle cerebral artery sign (HMCAS). The arterial occlusion site was definitively identified on cerebral angiography within two hours of the CT examination.
Results: LIR was present in 55% of patients with internal carotid artery occlusion. ALN was present in 65% of patients with occlusion of the sphenoidal portion (M1) of the middle cerebral artery. HSE was present in 47% of patients with middle cerebral artery branch occlusion. LIR was related independently to internal carotid artery occlusion (odds ratio (OR) 2.8 (95% confidence interval, 1.2 to 6.8)), ALN to M1 occlusion (OR 2.9 (1.2 to 7.4)), and isolated HSE without ALN or LIR to branch occlusion (OR 12.8 (3.2 to 51.5)). The combined presence of the three signs was indicative of internal carotid artery occlusion ($p < 0.05$), and the presence of ALN and LIR without HSE was indicative of M1 occlusion ($p < 0.05$) by univariate analysis. HMCAS bore no relation to either arterial occlusion site.
Conclusions: LIR, ALS, HSE, and combinations of these were useful predictors of the arterial occlusion site.

Although combined diffusion and perfusion weighted imaging has played an important role in the evaluation of acute stroke in recent years, computed tomography (CT) is still an essential imaging mode for the initial diagnosis of acute brain ischaemia in most institutes round the world.[1 2] In the first 24 hours after the onset of ischaemic stroke, CT does not reveal very much, but there are some important early abnormal signs, including loss of the insular ribbon (LIR),[3] attenuation of the lentiform nucleus (ALN),[4 5] hemispherical sulcus effacement (HSE),[3–5] and the hyperdense middle cerebral artery sign (HMCAS).[6 7] Following several studies on early CT signs in relatively small populations,[3–7] Moulin *et al* verified a strong correlation between these signs and subsequent infarct location in a study of 100 consecutive patients.[8]

The arterial occlusion site influences the outcome of thrombolytic treatment in the acute phase of stroke. Thrombolysis fails to recanalise acute occlusions of the internal carotid artery, and may increase the risk of haemorrhagic transformation.[9 10] However, intra-arterial infusion of recombinant prourokinase recanalised 66% of the middle cerebral artery occlusions, and improved the outcome of acute stroke caused by occlusions of that vessel.[11] Intravenous thrombolysis was also effective for middle cerebral artery occlusions occurring at the bifurcation or in the peripheral branch.[12] Thus prediction of the site of arterial occlusion at the time of initial diagnosis is very important for deciding the appropriate treatment strategy in the hyperacute phase.

Our aim in this study was to determine the value of early CT signs in predicting the arterial occlusion site in ischaemic strokes involving the anterior circulation, recruiting a consecutive series of patients in appropriate numbers.

METHODS

Between 1989 and 2000, 162 consecutive patients with acute embolic stroke involving the anterior circulation were admitted to St Mary's hospital, Kurume, Japan, and underwent cranial CT within six hours of stroke onset. Embolic stroke was defined on the basis of the criteria for cardiogenic brain embolism established by the Cerebral Embolism Task Force.[13] Fifty four patients who did not undergo cerebral angiography within two hours of their CT examination were excluded, as were three patients with isolated infarction in the territory of the anterior cerebral artery. Thus the final cohort included 105 patients.

Even in patients treated with intravenous thrombolysis, we generally carried out cerebral angiography. A cardiac or transcardiac embolic source was present in 86 patients. The remaining 19 had aortic or carotid arterial atheroma. Neurological deficits on admission were evaluated using the National Institutes of Health stroke scale (NIHSS).

Non-contrast cranial CT was done with a slice thickness of 10 mm, looking for infarcts or early CT signs (LIR, ALN, HSE, and HMCAS), according to definitions used in Moulin's previous study (fig 1).[8] Briefly, LIR was defined as decreased precision in delineating the grey-white interface at the lateral margin of the insula; ALN was defined as a decrease in density involving the lentiform nucleus area, including loss of precise delineation of the area; HSE was defined as decreased contrast density inducing a loss of precise delineation of the grey-white interface at the margins of the cortical sulci, corresponding to a localised mass effect; and HMCAS was defined as spontaneous high contrast in the middle cerebral artery. The findings were agreed between two stroke neurologists blinded to the patients' clinical features and to the results of the arteriogram. Both were familiar with neuroradiology.

Conventional angiography (n = 46) or digital subtraction angiography (n = 59) was done using transfemoral catheterisation. We divided the patients into three groups according to the arterial occlusion site: internal carotid artery occlusion; occlusion of the sphenoidal portion of middle cerebral artery (M1 occlusion); and occlusion of the middle cerebral artery at the bifurcation or the peripheral branch (branch occlusion).

Abbreviations: ALN; attenuation of the lentiform nucleus; HMCAS, hyperdense middle cerebral artery sign; HSE, hemispherical sulcus effacement; LIR, loss of the insular ribbon; NIHSS, National Institutes of Health stroke scale

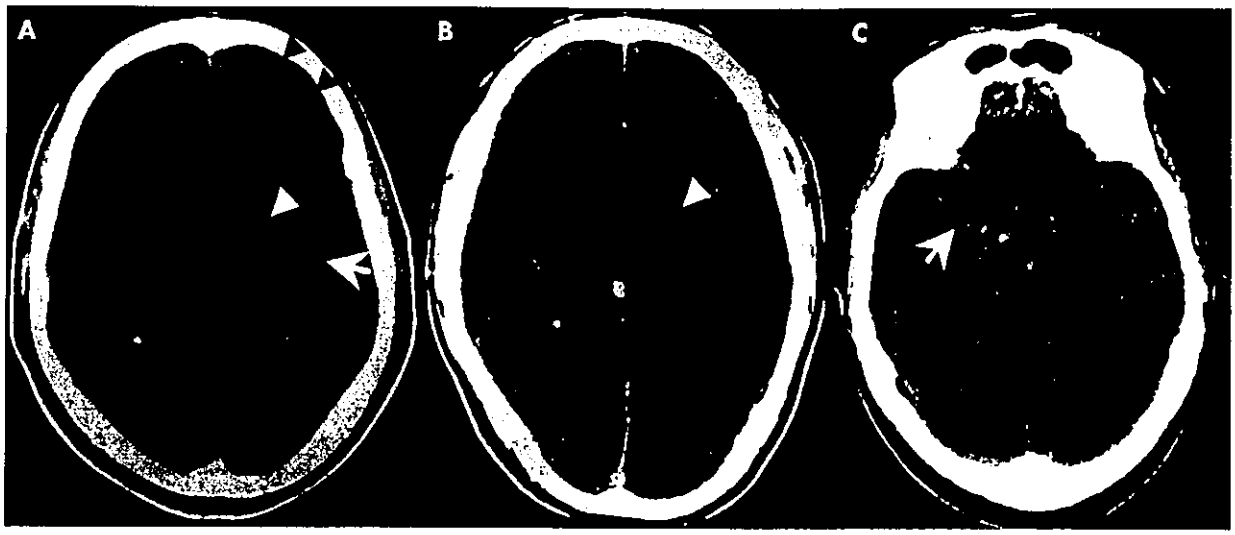

Figure 1 (A) Non-contrast brain computed tomography (CT) of a patient with embolic occlusion of the left internal carotid artery 2.5 hours after onset, showing loss of the insular ribbon (LIR, white arrow), attenuation of the lentiform nucleus (ALN, white arrowhead), hemispherical sulcus effacement (HSE, black arrowheads). (B) Non-contrast brain CT of a patient with embolic occlusion of the sphenoidal portion (M1) of left middle cerebral artery three hours after onset, showing ALN (white arrowhead). (C) Non-contrast brain CT of a patient with embolic occlusion of right M1 1.5 hours after onset, showing the hyperdense middle cerebral artery sign (HMCAS, white arrow).

Thrombolytic treatment was given to some patients within six hours of stroke onset.

We evaluated the following three indicators of therapeutic outcome in the patients: complete or partial recanalisation of the occluded artery documented on angiography one hour after thrombolysis; symptomatic or asymptomatic haemorrhagic transformation of the infarct documented on CT during the hospital admission; and modified Rankin scale score four weeks after stroke onset.

Statistics

Data are presented as mean (SD). In the univariate analysis, categorical variables were compared by the χ^2 test, continuous variables by an unpaired Student t test, and scoring variables by the Mann–Whitney U test. Multivariate analysis was done by logistic regression to identify the predictor variables for each arterial occlusion site. Differences were considered significant at a probability (p) value of < 0.05.

RESULTS

Sixty two men and 43 women aged 66 (10) years (range 42 to 80) were studied. Median NIHSS score on admission was 16 (range 3 to 30).

CT was undertaken at a mean of 112 (63) minutes (range 13 to 357) after stroke onset. ALN, LIR, or HSE, each indicating parenchymatous ischaemia, was present in 65 patients (62%). The prevalence of each of these three signs and their combinations is shown in table 1. HMCAS was present in 27 patients (26%), 23 of whom also had early parenchymatous signs. A fresh brain infarct was present in two patients (2%) and old infarcts in 32 (30.5%).

Angiography was done at a mean of 210 (68) minutes (range 55 to 410) after stroke onset (99 (48) minutes after CT). Internal carotid artery occlusion was present in 29 patients (28%), M1 occlusion in 34 (32%), and branch occlusion in 38 (36%).

LIR was the most frequent sign in patients with internal carotid artery occlusions (sensitivity 55%), ALN in those with

Table 1 Prevalence of early comuted tomographic signs and their association with the site of arterial occlusion

Sign	n	Prevalence	ICA (n=29)	M1 (n=34)	Branch (n=38)	No occlusion (n=4)
LIR, ALN, or HSE	65	62%	18 (62%)	25 (74%)	22 (58%)	0
LIR	39	37%	16 (55%)	16 (47%)	7 (18%)	0
ALN	43	41%	15 (52%)	22 (65%)	6 (16%)	0
HSE	43	41%	12 (41%)	13 (38%)	18 (47%)	0
LIR + ALN + HSE	20	19%	10 (34%)	8 (24%)	2 (5%)	0
LIR + ALN	14	13%	3 (10%)	8 (24%)	3 (8%)	0
LIR + HSE	3	3%	2 (7%)	0	1 (3%)	0
ALN + HSE	3	3%	0	2 (6%)	1 (3%)	0
Isolated LIR	2	2%	1 (3%)	0	1 (3%)	0
Isolated ALN	6	6%	2 (7%)	4 (12%)	0 (%)	0
Isolated HSE	17	16%	0	3 (9%)	14 (37%)	0
HMCAS	27	26%	10 (34%)	11 (32%)	6 (16%)	0
No sign	36	34%	10 (34%)	8 (24%)	14 (37%)	4 (100%)

Percentages in parentheses indicate sensitivity of early CT sign in each arterial occlusion group.
ALN, attenuation of the lentiform nucleus; branch, middle cerebral artery branch occlusion; CT, computed tomography; HMCAS, hyperdense middle cerebral artery sign; HSE, hemispherical sulcus effacement; ICA, internal carotid artery; LIR, loss of insular ribbon; M1, sphenoidal portion of the middle cerebral artery.

Table 2 Predictive factors for arterial occlusion site

	Sensitivity	Specificity	Accuracy	Univariate analysis, p value	Multivariate analysis, OR (95% CI)
			ICA occlusion		
Age ≥65 years	69%	34%	44%	NS	–
Male	59%	41%	46%	NS	–
NIHSS ≥16	62%	47%	51%	NS	–
LIR	55%	70%	66%	<0.05	2.8 (1.2 to 6.8)†
ALN	52%	63%	60%	NS	–
HSE	41%	59%	54%	NS	–
LIR+ALN+HSE	35%	87%	72%	<0.05	–
LIR+ALN	10%	86%	65%	NS	–
Isolated HSE	0%	78%	56%	<0.005*	–
HMCAS	35%	78%	66%	NS	–
			M1 occlusion		
Age ≥65 years	62%	31%	41%	NS	–
Male	62%	42%	49%	NS	–
NIHSS ≥16	79%	56%	64%	<0.001	3.4 (1.2 to 9.4)†
LIR	47%	68%	61%	NS	–
ALN	65%	70%	69%	<0.001	2.9 (1.2 to 7.4)†
HSE	38%	58%	51%	NS	–
LIR+ALN+HSE	24%	83%	64%	NS	–
LIR+ALN	24%	92%	70%	<0.05	–
Isolated HSE	9%	80%	57%	NS	–
HMCAS	32%	78%	63%	NS	–
			Branch occlusion		
Age ≥65 years	71%	36%	49%	NS	–
Male	58%	40%	47%	NS	–
NIHSS <16	66%	67%	67%	<0.005	5.0 (1.6 to 10.0)†
LIR	18%	52%	40%	<0.005*	–
ALN	16%	45%	34%	<0.0001*	–
HSE	47%	63%	57%	NS	–
LIR+ALN+HSE	5%	73%	49%	<0.01*	–
LIR+ALN	8%	84%	56%	NS	–
Isolated HSE	37%	96%	74%	<0.0001	12.8 (3.2 to 51.5)‡
HMCAS	16%	69%	50%	NS	–

*Significantly lower than the other occlusion groups.
†$p < 0.05$, ‡$p < 0.0005$.
Variables in bold have significance.
ALN, attenuation of the lentiform nucleus; branch, middle cerebral artery branch occlusion; HMCAS, hyperdense middle cerebral artery sign; HSE, hemispherical sulcus effacement; ICA, internal carotid artery; LIR, loss of insular ribbon; M1, sphenoidal portion of the middle cerebral artery; NIHSS, National Institutes of Health stroke scale.

M1 occlusions (sensitivity 65%), and HSE in those with branch occlusions (sensitivity 47%). Among combinations of these three signs, LIR+ALN+HSE seemed to indicate internal carotid artery occlusion (34%) or M1 occlusion (24%), LIR+ALN to indicate M1 occlusion (24%), and isolated HSE without LIR or ALN to indicate branch occlusion (37%). HMCAS seemed to indicate internal carotid artery occlusion (34%) or M1 occlusion (32%).

Possible predictive factors for arterial occlusion site were identified by univariate analysis for age, sex, NIHSS score, and the presence of each of the early signs alone or in combination (table 2). After multivariate analysis using the factors as independent variables, LIR was related independently to internal carotid artery occlusion (odds ratio (OR), 2.8 (95% confidence interval (CI), 1.2 to 6.8)); NIHSS score ≥ 16 (OR 3.4 (1.2 to 9.4)) and ALN (OR 2.9 (1.2 to 7.4)) to M1 occlusion; and NIHSS score < 16 (OR 5.0 (1.6 to 10.0)) and isolated HSE (OR 12.8 (3.2 to 51.5)) to branch occlusion. HMCAS, either alone or in combination with other signs, was not an independent indicator of any arterial occlusion site.

Thrombolytic treatment during the hyperacute stage of stroke was given in 81 patients, 52 intra-arterially and 29 intravenously; 25 were given tissue plasminogen activator (tPA) and 56 were given urokinase. Among these treated patients, 34 (42%) showed recanalisation of the occluded artery, 44 (54%) showed haemorrhagic infarction, and 29 (36%) showed good functional prognosis corresponding to a modified Rankin scale score of between 0 and 2. Arterial recanalisation was documented less often in patients with than without LIR ($p < 0.03$, table 3). Haemorrhagic infarction was more often found in patients with LIR ($p < 0.03$), ALN ($p < 0.02$), HMCAS ($p < 0.05$), or combinations of these signs ($p < 0.02$) than in patients without those signs. None of the CT signs was significantly correlated with good functional prognosis. The site of arterial occlusion in these 81 patients was internal carotid artery in 18 (62% of all patients with internal carotid artery occlusion), M1 in 32 (94%), and the middle cerebral artery branch in 31 (82%). Arterial recanalisation was documented in 22% of patients with internal carotid artery occlusion, in 44% of those with M1 occlusion, and in 52% of those with branch occlusion ($p > 0.1$); haemorrhagic infarction occurred in 72%, 69%, and 29%, respectively ($p < 0.001$); a good functional outcome was likely in 11%, 41%, and 45%, respectively ($p < 0.05$).

DISCUSSION

This is the first study on early CT signs as predictors of the arterial occlusion site in embolic stroke using a relatively large population. All parenchymatous signs and their combinations were useful for predicting internal carotid artery, M1, or branch occlusions. Our results assessing the vascular lesions causing infarction make a good contrast with those of Moulin *et al*,[8] who assessed subsequent infarcts.

Table 3 Correlation of early computed tomographic signs with therapeutic outcome

Early CT signs	n	Recanalisation (n=34)	Haemorrhagic infarction (n=44)	mRS 0-2 (n=29)
LIR	31	24% v 49% (p<0.03)	50% v 24% (p<0.03)	28% v 44% (NS)
ALN	36	32% v 53% (0.05<p<0.1)	57% v 30% (p<0.02)	38% v 48% (NS)
HSE	36	47% v 37% (NS)	52% v 35% (NS)	45% v 44% (NS)
LIR, ALN, or HSE	53	38% v 50% (NS)	64% v 36% (p<0.02)	36% v 36% (NS)
HMCAS	27	32% v 46% (NS)	36% v 16% (<0.05)	21% v 31% (NS)

Percentage of each therapeutic outcome between patients with and without CT signs.
ALN, attenuation of the lentiform nucleus; CT, computed tomography; HMCAS, hyperdense middle cerebral artery sign; HSE, hemispherical sulcus effacement; LIR, loss of insular ribbon; mRS, modified Rankin scale.

Loss of insular ribbon

The strong correlation between LIR and internal carotid artery occlusion in our present study is not in agreement with the suggestion in the original study[3] that LIR might result from middle cerebral artery occlusion distal to the lateral striate arteries. In contrast, the dominant appearance of extended infarcts in the middle cerebral artery territory in patients with LIR in Moulin's later study[8] appears to support our results to some extent. LIR hardly ever appeared alone in the present study, and more than half the patients with LIR also had ALN and HSE. The concomitant presence of these three signs also seemed to indicate internal carotid artery occlusion. After the European cooperative acute stroke study (ECASS) trial first indicated that hypoattenuation in more than 33% of the middle cerebral artery territory was a predictor of fatal outcome with thrombolytic treatment,[14] subsequent studies stressed this major early finding and paid little attention to LIR.[3 15 16] In contrast, the rt-PA stroke study group of the National Institute of Neurological Disorders and Stroke (NINDS) indicated that patients treated with tPA had a favourable outcome even if they had hypoattenuation in more than 33% of the middle cerebral artery territory.[17] Thus the diagnostic significance of this major early finding in relation to the use of thrombolysis is in dispute. Based on the present results, a combination of LIR and > 33% hypoattenuation of the middle cerebral artery territory may be a promising warning sign against the use of thrombolysis.

Attenuation of the lentiform nucleus

In the original studies,[4 5] all the acute stroke patients with angiographically proven internal carotid artery or M1 occlusion had ALN, presumably because the lentiform nucleus is fed by lenticulostriate arteries from M1 without collateral flow from cortical anastomoses. In the present study, ALN was also highly predictive of M1 occlusion, but was not present in all patients with this type of lesion. This might reflect the timing of CT. The presence of ALN in 16% of patients with branch occlusions appeared to result from variation in the lenticulostriate arteries, which arise from the middle cerebral artery branch in around 20% of cases.[18]

Hemispherical sulcus effacement

In contrast to LIR or ALN, HSE reflects cortical ischemia. Isolated HSE without LIR or ALN was highly indicative of branch occlusion in this study, and of a partial superficial infarct in the middle cerebral artery territory in the previous study.[8] Thus isolated HSE in stroke patients seems to be a good indication for intravenous thrombolysis.[12]

Treatment

Thrombolytic treatment was selected on the basis of the angiographic findings in this study. Many patients with internal carotid artery occlusion did not undergo thrombolysis. In spite of this selection bias, there were some interesting correlations between early CT signs and therapeutic outcome. Patients with LIR had poor arterial recanalisation, presumably because patients with internal carotid artery occlusion have a poor recanalisation rate and LIR has a strong correlation with internal carotid artery occlusion. Patients with HSE did not often have haemorrhagic infarction, presumably because patients with branch occlusion also did not often have haemorrhagic infarction, and HSE was strongly correlated with branch occlusion. The relatively small patient population related to the above mentioned selection bias may be the reason why early CT signs did not predict functional outcome in the chronic stage.

Limitations

Patients with high NIHSS scores on admission often failed to get their angiography within two hours after CT and so were excluded from the study. Internal carotid artery occlusion might well be the leading vascular lesion in these excluded patients, because this often causes large and fatal infarction in the middle cerebral artery territory.[19] Thus the exclusion of such patients may have affected our results with respect to internal carotid artery occlusion. The strong correlation of a high NIHSS score with M1 occlusion, but not with internal carotid artery occlusion, seems be a reflection of this possible bias. Another limitation of our results was that the sensitivity of each early ischaemic sign is rather low. In practical clinical situations, combining the information obtained from CT with, for example, carotid ultrasonography seems to be important for decisions about treatment in acute stroke. The CT analysts in this study were stroke specialists who were familiar with neuroradiology. However, even for experienced stroke specialists, there is considerable lack of agreement in recognising and qualifying the early CT changes.[20] Improvements in diagnostic methods for identifying early CT signs are expected. Finally, we should bear in mind that CT equipment upgrades over the 11 year period of the study may have introduced some differences in image quality that could have influenced our results.

Conclusions

A combination of early parenchymatous CT signs is important in predicting the arterial occlusion site in the acute stage of ischaemic stroke.

Authors' affiliations
M Koga, Y Saku, H Takaba, Division of Cerebrovascular Disorders, St Mary's Hospital, Kurume, Fukuoka, Japan
S Ibayashi, M Iida, Department of Medicine and Clinical Science, Graduate School of Medical Sciences, Kyushu University, Fukuoka
K Toyoda, Department of Cerebrovascular Disease, National Kyushu Medical Centre, Fukuoka

Competing interests: none declared

Correspondence to: Dr Kazunori Toyoda, Department of Cerebrovascular Disease, National Kyushu Medical Centre, 1-8-1 Jigyohama, Chuo-ku, Fukuoka 810-8563, Japan; toyoda@ qmed.hosp.go.jp

Received 26 April 2002
In revised form 9 October 2002
Accepted 15 January 2003

REFERENCES

1 **Barber PA**, Demchuk AM, Zhang J, *et al.* Validity and reliability of a quantitative computed tomography score in predicting outcome of hyperacute stroke before thrombolytic therapy. ASPECTS Study Group. Alberta Stroke Programme Early CT Score. *Lancet* 2000;**355**:1670–4.
2 **Grond M**, von Kummer R, Sobesky J, *et al.* Early x-ray hypoattenuation of brain parenchyma indicates extended critical hypoperfusion in acute stroke. *Stroke* 2000;**31**:133–9.
3 **Truwit CL**, Barkovich AJ, Gean-Marton A, *et al.* Loss of the insular ribbon: another early CT sign of acute middle cerebral artery infarction. *Radiology* 1990;**176**:801–6.
4 **Tomura N**, Uemura K, Inugami A, *et al.* Early CT finding in cerebral infarction: obscuration of the lentiform nucleus. *Radiology* 1988;**168**:463–7.
5 **Bozzao L**, Bastianello S, Fantozzi LM, *et al.* Correlation of angiographic and sequential CT findings in patients with evolving cerebral infarction. *Am J Neuroradiol* 1989;**10**:1215–22.
6 **Gács G**, Fox AJ, Barnett HJ, *et al.* CT visualization of intracranial arterial thromboembolism. *Stroke* 1983;**14**:756–62.
7 **Pressman BD**, Tourje EJ, Thompson JR. An early CT sign of ischemic infarction: increased density in a cerebral artery. *Am J Roentgenol* 1987;**149**:583–6.
8 **Moulin T**, Cattin F, Crépin-Leblond T, *et al.* Early CT signs in acute middle cerebral artery infarction: predictive value for subsequent infarct locations and outcome. *Neurology* 1996;**47**:366–75.
9 **Jansen O**, von Kummer R, Forsting M, *et al.* Thrombolytic therapy in acute occlusion of the intracranial internal carotid artery bifurcation. *Am J Neuroradiol* 1995;**16**:1977–86.
10 **Jahan R**, Duckwiler GR, Kidwell CS, *et al.* Intraarterial thrombolysis for treatment of acute stroke: experience in 26 patients with long-term follow-up. *Am J Neuroradiol* 1999;**20**:1291–9.
11 **Furlan A**, Higashida R, Wechsler L, *et al.* Intra-arterial prourokinase for acute ischemic stroke. The PROACT II study: a randomized controlled trial. Prolyse in acute cerebral thrombpembolism. *JAMA* 1999;**282**:2003–11.
12 **del Zoppo GJ**, Poeck K, Pessin MS, *et al.* Recombinant tissue plasminogen activator in acute thrombotic and embolic stroke. *Ann Neurol* 1992;**32**:78–86.
13 **Cerebral Embolism Task Force.** Cardiogenic brain embolism. *Arch Neurol* 1986;**43**:71–84.
14 **Hacke W**, Kaste M, Fieschi C, *et al.* Intravenous thrombolysis with recombinant tissue plasminogen activator for acute hemispheric stroke. The European Cooperative Acute Stroke Study (ECASS). *JAMA* 1995;**274**:1017–25.
15 **von Kummer R**, Allen KL, Holle R, *et al.* Acute stroke: usefulness of early CT findings before thrombolytic therapy. *Radiology* 1997;**205**:327–33.
16 **Kucinski T**, Koch C, Grzyska U, *et al.* The predictive value of early CT and angiography for fatal hemispheric swelling in acute stroke. *Am J Neuroradiol* 1998;**19**:839–46.
17 **Patel SC**, Levine SR, Tilley BC, *et al.* Lack of clinical significance of early ischemic changes on computed tomography in acute stroke. *JAMA* 2001;**286**:1830–8.
18 **Jain KK.** Some observations on the anatomy of the middle cerebral artery. *Can J Surg* 1964;**7**:134–9.
19 **Heinsius T**, Bogousslavsky J, van Melle G. Large infarcts in the middle cerebral artery territory: etiology and outcome patterns. *Neurology* 1998;**50**:341–50.
20 **Gratta JC**, Chiu D, Lu M, *et al.* Agreement and variability in the interpretation of early CT changes in stroke patients qualifying for intravenous rtPA therapy. *Stroke* 1999;**30**:1528–33.

AJNR Am J Neuroradiol 24:886–891, May 2003

Ultrasonographically Predicting the Extent of Collateral Flow through Superficial Temporal Artery-to-Middle Cerebral Artery Anastomosis

Shuji Arakawa, Masahiro Kamouchi, Yasushi Okada, Kazuhiro Kishikawa, Tsuyoshi Omae, Tooru Inoue, Setsuro Ibayashi, and Masatoshi Fujishima

BACKGROUND AND PURPOSE: **This study was performed to elucidate whether the extent of bypass flow through superficial temporal artery-to-middle cerebral artery (STA-MCA) anastomosis could be indirectly estimated by measuring the blood flow velocity in the superficial temporal artery (STA) by using duplex ultrasonography.**

METHODS: **We analyzed 29 patients (31 sides) who underwent STA-MCA bypass surgery for occlusive cerebrovascular disease (28 sides) or unclippable cerebral aneurysm that required therapeutic occlusion of the internal carotid artery (three sides). The flow velocities of the STA were measured by using ultrasonography. For patients who underwent the surgery unilaterally, the flow velocity ratios of the operated side to the contralateral side for the individual arteries were calculated. The correlation between these flow velocity parameters and the extent of bypass flow, which was graded based on the findings of cerebral angiography, was investigated.**

RESULTS: **Both the affected STA flow velocity and the STA flow velocity ratio, particularly those in the end diastole, increased in patients with more extensive bypass flow. In patients with extensive, moderate, and poor bypass flow, the end diastolic flow velocities of the operated STA were 27.4 ± 8.8, 23.0 ± 7.8, and 13.5 ± 7.5 cm/s, respectively and the end diastolic flow velocity ratios of the STA were 3.4 ± 0.8, 2.1 ± 0.5 and 1.3 ± 0.4, respectively. The pulsatility index and resistance index of the affected STA were significantly lower in the patients with more extensive bypass flow. The optimal threshold value of the end diastolic flow velocity ratio of STA for the group with extensive bypass flow was 2.75, whereas that for the group with poor bypass flow was 1.60. With the obtained values, the sensitivity and specificity were 87.5% and 93.9% for the group with extensive bypass flow and 95.2% and 95.0% for the group with poor bypass flow, respectively.**

CONCLUSION: **The blood flow velocity in the operated STA seems to be a highly sensitive parameter for predicting the extent of bypass flow in patients undergoing STA-MCA anastomosis.**

Superficial temporal artery-to-middle cerebral artery (STA-MCA) bypass is a direct type of revascularization surgery that was pioneered by Yasargil et al (1) and has been applied to moyamoya disease (2). It is now generally accepted that this direct revascularization surgery seems to provide a remarkable improvement in cerebral blood flow and a better prognosis than that associated with conservative treatment. This procedure has also been used in patients who require therapeutic occlusion of the internal carotid artery for unclippable cerebral aneurysms or certain skull base tumors (3, 4). In patients with atherosclerotic arterial disease in the carotid arteries and middle cerebral arteries (MCAs), however, a 1985 Cooperative Study reported an extracranial-intracranial bypass to be ineffective in preventing cerebral ischemia (5). Although the results of this trial caused many physicians to abandon the procedure, additional studies indicate that this technique may improve the effect of surgical therapy for internal carotid artery occlusion (6–9).

Received October 21, 2002; accepted after revision November 26.

This work was supported by cardiovascular research grants 12A-2 and 12C-10 from the Ministry of Health, Labor and Welfare of Japan.

This work was presented in part at the 4th World Stroke Congress, Melbourne, Australia, November 25–29, 2000.

From the Departments of Cerebrovascular Disease (S.A., M.K., Y.O., K.K., T.O.) and Neurosurgery (T.I.), Clinical Research Institute, National Kyushu Medical Center; and the Department of Medicine and Clinical Science (M.K., S.I., M.F.), Graduate School of Medical Sciences, Kyushu University, Fukuoka, Japan.

Address reprint requests to Shuji Arakawa, MD, Department of Medicine and Clinical Science, Graduate School of Medical Sciences, Kyushu University, Maidashi 3-1-1, Higashi-ku, Fukuoka 812-8582, Japan.

Clinical characteristics of the patients and controls

	Patient	Control
No. of cases (sides)	29 (31)	15
Mean age, y	64.4 ± 9.9	68.6 ± 8.7
Sex, M/F	23/6	9/6
Clinical diagnosis		
ICA/MCA occlusive disease	26 (28)	
Unclippable cerebral aneurysm	3 (3)	

Note.—ICA indicates internal carotid artery; MCA, middle cerebral artery.

Recently, Grubb et al (10) indicated that stage II hemodynamic failure defines a subgroup of patients with symptomatic carotid occlusion who are at high risk for subsequent stroke when treated medically. Considering that the Cooperative EC/IC Bypass Study lacked an assessment of the collateral circulation and cerebrovascular reserve, a randomized trial evaluating surgical revascularization in this high risk subgroup seems called for. In Japan, a multicenter randomized re-trial including strictly selected patients is currently in progress (Japan EC-IC Bypass Trial: JET Study) (11, 12).

After STA-MCA anastomosis, the patients were required to undergo postoperative selective angiography to confirm the patency and extent of improved filling of the affected MCA branches. The luxuriance of the bypass could be directly evaluated by the number and size of the branches opacified from the donor STA compared with the preoperative appearance. However, angiography is an invasive procedure associated with non-negligible complications and should not be repeatedly performed as a follow-up study. Because of these limitations, noninvasive and easily repeatable techniques are preferable. The present study was thus designed to examine whether the extent of bypass flow could be estimated by duplex ultrasonography. We measured the postoperative flow velocities of STA and compared them with the findings of cerebral angiography. We herein present the first report of the predictable value of ultrasonography in clarifying the extent of the collateral flow through the bypass.

Methods

Participants

The study participants consisted of 29 consecutive patients (31 sides) who underwent STA-MCA anastomosis and were examined with the use of postoperative cerebral angiography and duplex ultrasonography. Both tests were performed simultaneously 1 month after surgery. The average age of the patients (23 men, six women) was 64.4 years. STA-MCA anastomosis was performed for 26 patients (28 sides) with internal carotid artery/MCA occlusive disease and three patients (three sides) each with an unclippable cerebral aneurysm that required therapeutic occlusion of the internal carotid artery. The clinical characteristics of the patients and control participants are summarized in the Table. The selection criteria for STA-MCA anastomosis in the patients with internal carotid artery/MCA occlusive disease was identical to that used in a JET study (11, 12). All patients with atherosclerotic internal carotid artery/MCA occlusive disease underwent stimulated cerebral blood flow study preoperatively and all showed impairment of the perfusion reserve. Surgery was performed with the patients under general anesthesia. Blood pressure, heart rate, blood gas, and an electric potentials of the brain were continuously monitored during the procedure. All patients provided informed consent to be treated with this surgical method and to be examined by these tests.

Techniques

Ultrasonography was performed by a neurosonographer, who was blinded to the angiographic information, using a color-coded duplex ultrasonographic device (LOGIQ500MD; GE Yokogawa Medical Systems Ltd., Tokyo, Japan). A 5.0- to 10.0-MHz and a 5.0-MHz sonography beam were used for imaging and pulsed Doppler sonography, respectively. For the examinations of STA, each patient was examined in a supine position with his or her head turned away from the side undergoing imaging. The transducer was placed in the temporal region before the external opening of the acoustic canal, and STA underwent color imaging. On the longitudinal images, the sample volume was set within the STA at the point proximal to its bifurcation. Particular care was taken to keep the incident angle between the beam and the STA at ≤60 degrees. The peak systolic velocity (PSV), end diastolic velocity (EDV), and time-averaged mean velocity (TMV) were measured in both STAs and were then corrected with the incident angle. The flow velocities of the external carotid artery (ECA) were also measured. The pulsatility index (PI) and resistance index (RI) for the individual arteries were calculated by using the following formulae: PI = (PSV-EDV)/TMV and RI = (PSV-EDV)/PSV.

To obtain normal values, 15 age-matched control participants who had never suffered a stroke and had no major cerebral artery occlusive disease underwent ultrasonographic examinations (nine men, six women; average age at examination, 68.6 years). To avoid any influence of systemic factors, we calculated the flow velocity parameter ratios of the operated side to the contralateral side for the patients who underwent the surgery unilaterally. For the control participants, the flow velocity parameter ratio of the higher side in EDV of the STA to the contralateral side was obtained.

Conventional selective angiography was performed by a neuroradiologist. The pattern of the collateral circulation through the bypass was categorized based on postoperative external carotid angiograms. We graded the extent of bypass flow without any knowledge of ultrasonographic findings. Three categories were determined based on postoperative angiograms as follows: extensive, antegrade and retrograde filling of the entire MCA system; moderate, filling of two or more MCA branches; and poor, filling of only the anastomosed MCA branch.

Statistical Analysis

All data were expressed means ± SD. Statistical comparisons between the groups were performed with analysis of variance and then Scheffe's multiple comparison test. The cutoff values of the STA flow velocity parameters for predicting each group were analyzed with a sensitivity-specificity curve analysis. A value of $P < .05$ was considered to indicate a statistically significant difference.

Results

Postoperative Angiographic Findings

The patients were divided into three groups based on the pattern of the collateral circulation through the bypass, which was determined based on the angiographic findings. They consisted of an extensive